Control of oscillatory thermocapillary convection

by

Junichiro Shiomi

December 2003 Technical Reports from Royal Institute of Technology Department of Mechanics SE-100 44 Stockholm, Sweden

	Typsatt i $\mathbb{I}\!\!\!\!/ T_{\!E\!} X$ med mekaniks avhandlingsstil.
Λ1.	ademisk avhandling som med tillstånd av Kungliga Tekniska Högskola
Sto	ockholm framlägges till offentlig granskning för avläggande av teknologie ocknom fredagen den 5:e December 2003 kl 10.15 i Kollegiesalen, Adnationsbyggnaden, Kungliga Tekniska Högskolan, Valhallavägen 79, Sto
©	Junichiro Shiomi 2003
Un	iversitetsservice US AB, Stockholm 2003



Control of oscillatory thermocapillary convection Junichiro Shiomi 2003

Department of Mechanics, Royal Institute of Technology SE-100 44 Stockholm, Sweden

Abstract

The possibility to stabilize the oscillatory thermocapillary convection is demonstrated using a proportional feedback control. This topic has a strong industrial motivation in connection with a container-less crystal growth method called the floating-zone technique. The thermocapillary oscillation is known to cause detrimental striations, microscopic inhomogeneity of the dopant distribution, in the final product of the crystal growth process. The feedback control is realized by locally modifying the surface temperature by using the local temperature measured at different locations fed back through a simple control law. Placing sensor/actuator pairs (controllers) in a strategical manner using the knowledge of the modal structures, a simple cancellation scheme can be constructed with only a few controllers. In this method, the state can be stabilized without altering the base flow appreciably which could be advantageous compared with other available control methods targeting the base convection.

As an initial study of such kind of control method, this thesis work explores the possibility of applying the control in simplified geometries such as the annular configuration and the half-zone for high Prandtl number liquids by means of experiments, numerical simulations, and formulation of a simple model equation system. Successful suppression of the oscillation was obtained especially in the weakly nonlinear regime where the control completely suppresses the oscillations. With a right choice of actuators, even with the local control, it was shown that it is possible to modify the linear and weakly-nonlinear properties of the three-dimensional flow system with linear and weakly nonlinear control. On the other hand, the method exhibits certain limitations. Depending on the geometry of the system and actuators, the limitation can be caused by either the enhancement of nonlinear dynamics due to the finite size of the actuators or the amplification of new linear modes. The former case can be attenuated by increasing the azimuthal length of the actuators to reduce the generation of broad wavenumber waves. In the latter case, having an idea of the structures of the newly appearing modes, the destabilization of those modes can be delayed by optimizing the configuration of controllers. On the whole, the oscillation can be attenuated significantly in a range of supercritical Ma up to almost twice the critical value.

Descriptors: Fluid mechanics, Marangoni convection, thermocapillary convection, annular configuration, half-zone, feedback control, flow visualization, low dimensional model, bifurcation.

Preface

This thesis contains the study of feedback control of oscillatory thermocapillary convection by modification of local temperature field on the free surface. The first part consists of the introduction to the field of study and the summary of the research presented in the papers. The second part of the thesis is composed of the following papers.

- **Paper 1.** Shiomi, J., Amberg, G. & Alfredsson, H. 2001 Active control of oscillatory thermocapillary convection. *Physical Review E*, **64**, 031205
- **Paper 2.** Shiomi, J. & Amberg, G. 2002 Active control of a global thermocapillary instability. *Physics of Fluids*, **14**, pp. 3039–3045
- **Paper 3.** Shiomi, J., Kudo, M., Ueno, I., Kawamura, H. & Amberg, G. 2003 Feedback control of oscillatory thermocapillary convection in a half-zone liquid bridge. *Journal of Fluid Mechanics*, **496**, pp. 193–211
- **Paper 4.** Shiomi, J. & Amberg, G. 2003 Proportional control of oscillatory thermocapillary convection in a toy model. To be submitted.
- **Paper 5.** Bárcena, L., Shiomi, J. & Amberg, G. 2003 Control of thermocapillary instability with local heating. To be submitted.
- **Paper 6.** Shiomi, J. & Amberg, G. 2003 Numerical investigation of feedback control of thermocapillary instability. To be submitted.

Division of work between paper authors

The works presented in Paper 1, 2, 4 and 6 were performed and documented by Junichiro Shiomi (JS) with supervision of Gustav Amberg (GA).

Paper 3 is the result of collaborative research with Tokyo University of Science (TUS), Chiba, Japan. The experiment was conducted in TUS using their half-zone facility. The experiment was mainly performed by JS and Masaki Kudo (MK) and documented by JS with help from MK, Ichiro Ueno, Hiroshi Kawamura and GA.

Paper 5 is based on the Mater's thesis work of Luis Bácerna (LB). The experiment was performed and documented by LB with guidance of JS. The paper was revised by JS.

Contents

Preface		vii
Divisio	n of work between paper authors	viii
Part 1.	Summary	1
Chapter	1. Introduction	3
Chapter	2. Oscillatory thermocapillary convection	6
2.1. I	Cloating-zone technique	6
2.2.	Simplified geometries	8
2.3. I	Half-zones	10
2.4. A	Annular configuration	12
Chapter	3. Basic concepts	15
3.1.	Governing equations	15
3.2.	caling analysis	17
3.3. N	Modal structures	19
3.4. V	Veakly nonlinear analysis	21
3.5. I	Bifurcation theory	23
3.6. I	Routes to chaos	24
Chapter	4. Active control of thermal convection	26
4.1.	Control of natural convection	26
4.2.	Control of steady thermocapillary convection	27
Chapter	5. Methodologies	30
5.1. (Opposition control	30
5.2. V	Veakly nonlinear control	30
5.3. I	Experiments	31
54 7	Toy model formulation	35

x CONTENTS

5.5.	Numerical simulations	36
Chapte	er 6. Summary of results	38
6.1.	Single actuator control	38
6.2.	Global suppression of the oscillation	38
6.3.	Limitations of control	39
6.4.	Remedies	42
6.5.	Bifurcation characteristics of the controlled system	42
6.6.	Controlling the period-doubling oscillation	43
6.7.	Overall performance	43
Chapte	er 7. Conclusions and outlook	45
Ackno	wledgment	48
Bibliog	graphy	49



Part 1 Summary

CHAPTER 1

Introduction

Free surface flows are omnipresent in nature with practical importance in diverse situations. The surface tension phenomena are also in charge of some of the *curious* fluid motions we encounter in our everyday life. A familiar example is the *tears of wine*, also known as the *leg* of wine, a traditional measure to check the character of the wine. In a glass of wine, there is a accumulation of wine in a band on the top edge of the thin film of wine some distance up from the surface. From this band, *tears*, drops of the wine, are released and flow back into the bulk of wine leaving steaks along the side of the glass.

If you looked at a glass of water on the other hand, you would realize that the glass of water does not cry. The tears of wine result from the evaporation of alcohol in wine. In the thin film of wine along the side of the glass, more evaporation of alcohol results in lower alcohol concentration. Since the surface tension of water is higher than that of alcohol, variations in concentration give rise to gradients of surface tension. Consequently, the wine is drawn up along the side of the glass, until it breaks into tears due to the gravitational force. This phenomenon was first correctly explained by Thomson (1855) and today, studies are available with more thorough analyses of the physics (Vuilleumier et al. 2001; Hosoi & Bush 2001).

This type of convection was named after Carlo Marangoni (1840–1925) who first suggested that a flow can be driven by the surface tension gradient not only due to the variation in the composition, but also the variation in the temperature. The Marangoni convection caused by temperature variation is often addressed as thermocapillary convection. The Marangoni number (Ma), which describes the ratio of heat transport and thermal diffusion, is often used to indicate the strength of the driving force.

As described in the earliest review of Scriven & Sternling (1960), there are tremendous number of situations were the Maragoni effect has practical importance in industrial applications. Especially, the Maragoni convection can be seen in many of material processing situations involving melting and solidification which give rise to the interface of two immiscible fluids subjected to a temperature gradient. For example, in the semiconductor crystal growth and welding processes, the thermocapillary convection has a significant influence on the quality of the finished product.

4 1. INTRODUCTION

In a crystal growth method called floating-zone technique, the time dependent state of the convection is blamed for detrimental striations in the chemical composition of the finished crystal. The industrial need has motivated a number of theoretical, experimental and numerical studies to clarify the onset mechanism of the instability and the structure of the resulting oscillation. Many studies on the convective flow were carried out in various simplified model problems where generic convection similar to that of the flow in the floating-zone melt is realized. Recently, further development in the field of study has contributed on understanding important characteristics of supercritical behavior of the oscillatory flows. Most of the ground-based experiments are carried out in geometries with scales of several millimeters in order to have thermocapillary forces dominant over buoyancy forces. With the demand for experiments in micro-gravity conditions, this problem has been caught in the limelight as a candidate for space-based projects.

Based on the knowledge obtained from these extensive researches, the ultimate goal of this field of study would be to stabilize the instability to improve the quality of semiconductors. In the industries, the control problem of the crystal growth process has been around for years. For example, in the floating-zone technique with radio frequency heating, because of the asymmetric thermal field of the radio frequency coil, the growing crystal is subjected to a rotation to obtain a symmetric single crystal. The rotation is also often applied to the system to maintain the cylindrical shape of the melted zone. Since the oscillatory state of the convection was found to be the prior cause of the detrimental striation, the microscopic inhomogeneity of dopant and impurity distribution, in the finished product, there has been an increasing interest in suppression of the oscillation. Most of the works done thus far aim to reduce or alter the steady state, in other word, to decrease the effective Ma, and thus to attenuate the fluctuation. For example, a well known method is to apply a magnetic field to an electronically conductive melt. Others are counteracting the surface flow by generating a stream by end-wall vibration or directing a gas jet parallel to the surface. A drawback of these methods is that the damping of the base convection enhances the macro-segregation of the chemical compositions due to the weakening of the global mixing.

An alternative way to attenuate the oscillation would be to act only on the thermocapillary instability. If one could stabilize the instability without influencing the base flow appreciably, it might be beneficial in terms of both microscopic and macroscopic homogeneity of the final single crystal. When it comes to this type of method to control the oscillatory thermocapillary convection, there has been only a limited number of works reported. The idea originates in that if the surface temperature distribution plays a key role in the instability mechanism, the property of the oscillation should be able to be altered by modification of the temperature. The objective is to suppress only the fluctuation without altering the base flow by modifying the stability characteristics. Knowing the structure of the oscillation, a few sensors and actuators are strategically positioned to realize the feedback control. With the help of feedback control, an attempt can be made to minimize the cost of control.

The attraction of the current study in the academic point of view should also be noted. This problem contains rich fundamental physics with nonlinear dynamics which can lead the flow to chaotic states. At the same time, the problem has a few advantages to be subjected for active flow control. Firstly, since only a limited number of spatial modes play a role in the instability, the flow can be possibly controlled with a small number of controllers. Secondly, the flow can be altered by modifying the temperature which is usually experimentally accessible. Finally, being a rather slow phenomenon compared to other popular targets of flow control, for instance flows on airfoils, the instability could be a suitable target for a control scheme which involves real-time computation of system equations.

CHAPTER 2

Oscillatory thermocapillary convection

2.1. Floating-zone technique

In crystal growth, taking advantage of the difference in melting and freezing points of various components, a poly-crystal material, can be refined by melting and freezing the material. Among various refining techniques in the production of single crystals, a container-less processing called floating-zone technique has advantages to increase the purity of the crystal (Pfann 1966; Zief & Wilcox 1967). When refining materials which are reactive when melted, such as silicon, it is difficult to obtain high purity by processing it in containers.

In the floating-zone technique, a raw material rod is slowly pulled through a ring heater, and the small zone near the heater is melted and re-solidified as the heater passes by (figure 2.1). Impurities travel with the molted zone, therefore purifying the remainder. The melted zone is held in place by surface tensions between two vertical solid rods. Axial rotation is often applied to the rod to maintain the cylindrical shape of the melt.

The flow in the melt has a strong influence on the quality of the finished crystals in terms of purity and uniformity. It also influences the stability and shape of the melt. The possible driving sources of convection are gravitational buoyancy forces, thermocapillary forces and electromagnetic forces due to induction heating which can be avoided by applying a radiative heating instead. Since the system has been proposed for space processing in order to minimize the influence of the gravitational convection, many works have been focused on the influence of thermocapillary convection.

Among the problems associated with the floating-zone technique, the development of microscopic striations in the single crystals, the regions of varying concentration of impurities or dopants, is known to cause an inhomogeneous material property distribution in the final product. The striations can be observed in the refined single crystal as a pattern shown in figure 2.2.

2.1.1. Crystal growth experiments

In many early studies of the actual crystal growth of silicon or metals, the influence of convective transport phenomena in the melt were indirectly deduced from analyses of the striations in the grown crystal. Experiments were

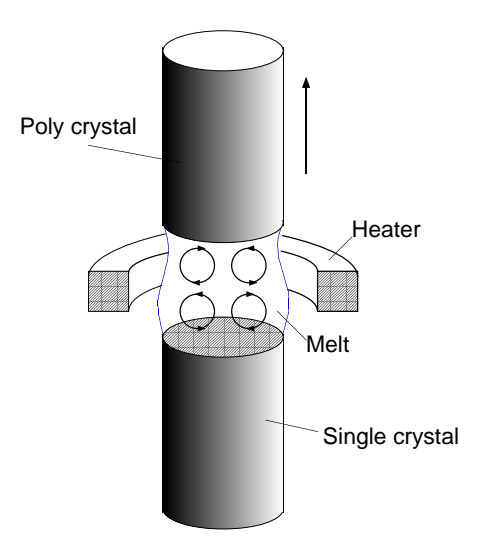


FIGURE 2.1. Floating-zone technique

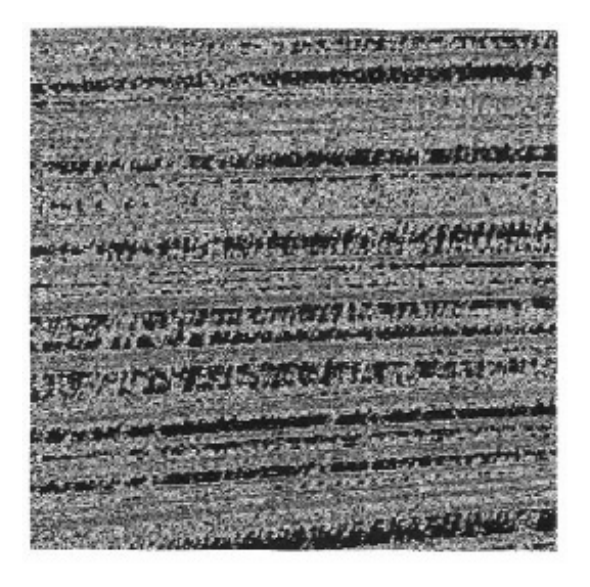


FIGURE 2.2. Striation: inhomogeneities of the dopant distribution in refined crystals

performed in normal gravity and also in microgravity conditions where the thermocapillary force was dominant over other sources of convection (Eyer *et al.* 1985; Cröll *et al.* 1991). Consequently, similar striation patterns were observed

for both cases, which suggested that the thermocapillary convection is responsible for the dopant striations in silicon crystals, though they have also observed a non-trivial difference in terms of the instensity of the resulting strictions. Jurisch & Löser (1990) and Cröll et al. (1989) examined the striction patterns for various strength of the thermocapillary convection in floating-zones of molybdenum and silicon, and observed that the striations appear above a well-defined critical physical condition. It was suggested that the time-dependent oscillatory state of the thermocapillary convection was the cause for the detrimental striations in the chemical composition of the single crystal. This was confirmed by Jurisch (1990) who measured the surface temperature of stationary molybdenum float-zones and observed the oscillations whose frequencies matched the analyses of the striations seen in the grown crystal. More temperature measurements in actual crystal growth are available at this date. For floating-zone silicon melts, the temperature oscillations have been measured by an optical fiber thermometry (Schweizer et al. 1999) and by non-intrusive techniques such as phase-shift Michelson interferometry (Hibiya et al. 2002). However, owing to the complexity of the system and the experimental inconvenience of handling the low Prandtl number (Pr) liquids, experimental analyses of the internal flow and temperature fields and parameter studies for characterizing the instability encounter severe difficulties.

2.1.2. Flow analyses in floating-zones

Most of the observations of the flow in the floating-zone are done by either numerical simulations or experiments using high Pr liquids. These are commonly carried out in a stationary floating-zone model, where the melt is fixed at the same location without any rotation to the system for simplicity. Main challenge of the early works were to characterize the two-dimensional basic flow. When only thermocapillary force is considered, there will be two vortices forming on top of each other as shown in figure 2.1. Since, in most of liquids, the surface tension decreases with temperature, the flow is driven from the mid-hight of the melt to the solid-liquid boundaries on the free surface. The first works to examine the flow in the floating-zone melt was done by Chang & Wilcox (1976) using a numerical simulation. The flow pattern and temperature distribution were simulated for a cylindrical silicon melt. Later, Schwabe & Scharmann (1979) carried out an experiment in a floating-zone apparatus and observed similar flow patterns. Kazarinoff & Wilkowski (1989, 1990) made numerical simulations of a two-dimensional axisymmetric full float-zone. They discussed the possibility for two-dimensional time-dependent flow and demonstrated its bifurcation scenario.

2.2. Simplified geometries

In general, the full floating-zone geometry introduces complexity to the problem especially for three-dimensional oscillatory flows. Therefore many of the reported flow studies were carried out in simplified geometries. Since the first experimental observations of the three-dimensional time-dependent state in thermocapillary convection by Schwabe & Scharmann (1979) and Chun & Wuest (1979) in one of the simplified models called the half-zone, the main interest in this field shifted towards the physics of the time-dependent oscillatory convection. Many of the experimental studies deal with high Pr flow $(Pr \gg 1)$ which is easier to handle compared with low Pr liquids $(Pr \ll 1)$. A review of the recent experimental works in this field is documented by Schatz & Neitzel (2001). For flows with low Pr fluid, contributions are mostly done by means of numerical simulations.

2.2.1. Shallow liquid layers

2.2.1.1. Classical Marangoni convection

Most of the early theoretical analyses of thermocapillary instabilities were done in thin liquid layers. The classical problem is the Marangoni convection in a static liquid layer heated from below. The linear stability analysis was demonstrated by Pearson (1958) who showed that many of the reported cells in Rayleigh-Benard convection flows were in fact caused by the surface tension force. The mechanism for this instability is simple. First, we consider a hot spot on the free surface. This drives a flow outwards from the hot spot due to the surface tension. At the same time, due to the continuity, the internal fluid is driven upward to the surface. Since the internal fluid is warmer than that on the surface, the process is amplified. The outward flow from the hot spot travels until it reaches the edges of the cell and descends towards the bottom surface to maintain the circulation.

2.2.1.2. Hydrothermal wave

Departing from the rather ideal case with a temperature gradient perpendicular to the free surface, Smith & Davis (1983) described the onset of the convection with interfacial motions driven by the temperature gradient parallel to the free surface. This simple case, originally invented for realization of a theoretical analysis, is an important model where the insights on the instability mechanism in more complicated geometries can be gained. Two types of base flow were tested, one with a linear velocity profile, and the other with a return flow in the bottom of the cavity. In addition to the stationary longitudinal rolls driven by the similar mechanism as the classical Marangoni layer heated from below, a new type of instability, which takes a form of propagating temperature disturbance, was identified. For the return flow, this convective instability named hydrothermal-wave instability is the primary instability independently of Pr. The temperature disturbance wave was found to propagate in different directions for low and high Pr liquids. Later, this problem was experimentally

realized by Riley & Neitzel (1998) in a finite shallow liquid layer with a horizontal temperature gradient using high Pr fluid and the hydrothermal-wave instability was successfully detected.

2.2.1.3. Physical explanation of the hydrothermal wave

The physical interpretation for the mechanism of the hydrothermal wave instability was given by Smith (1986). Being a more complicated problem than the classical Marangoni convection, the full description of the scenario tends to be rather lengthy and here only the key points for the case with closed ends are reviewed. The mechanism is different for low and high Pr since, in the range of the critical Marangoni number (Ma_{cr}) obtained in Smith & Davis (1983), the flow is conductive-inertial and convective-viscous dominated, respectively.

One of the distinct feature of the hydrothermal wave compared with the classical Marangoni convection with vertically imposed temperature gradient is that it takes the form of an oscillation. This means that there needs to be a mechanism which changes a hot spot to a cold spot and vice verse. The oscillation is sustained by a sequence of overshoots of one effect being damped by the other.

In the low Pr limit, this can be understood by considering the dominating inertial effect. Consider a hot spot on the free surface in the form of a line in the streamwise-direction in figure 2.3(a). Just as in the classical Marangoni mechanism, outward-spanwise flow and up-flow is driven as a result of thermocapillarity and continuity. Because of the existing velocity shear, the upflow brings fluid with a lower velocity up to the free surface. This creates an inertial force which drives the upsteam velocity perturbation. The upstream carries cold fluid and reduces the temperature of the spot. The lag in the viscous and conductive time scales causes the overshoot of the cooling, and hence the cold spot appears. Note, with this explanation, the flow cannot be entirely conductive, since certain convection would be needed cool the spot. The transition back to a hot spot takes the reversed manner.

The scenario may be intuitively simpler for high Pr, where the wave is driven by heat transport coupled with thermocapillarity. This time, the growing perturbation takes the form of a line in the spanwise-direction. Just as in the case of low Pr, the upflow is driven at the hot spot which carries up cold internal fluid and cools the spot. The opposite is basically the same; the cold spot drives the downstream flow carrying the hot fluid. Due to the convective nature of the flow, the resulting internal hot spot is carried downstream by the internal mean flow.

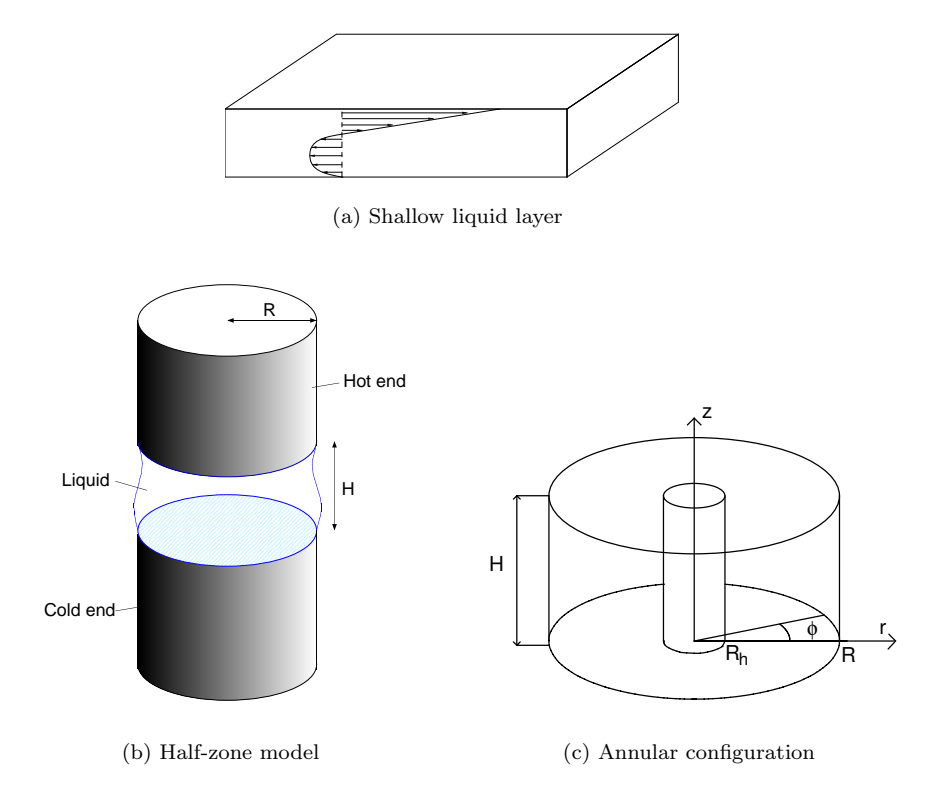


Figure 2.3. Various simplified geometries

2.3. Half-zones

Many of the recent studies have been carried out for a simplified model geometry called the half-zone model, which essentially models half of the floating-zone. In a half-zone, as shown in figure 2.3(b), a liquid drop is held by surface tension forces between two coaxial rods maintained at different temperatures to impose an axial temperature gradient on the free surface. On increasing the temperature difference imposed between the top and bottom rod above a certain value, the flow becomes time dependent exhibiting an oscillation with a distinct azimuthal wavenumber. The most dangerous wavenumber and the critical frequency have a strong dependence on the geometrical parameters, mainly the aspect ratio, A_r , the ratio of the hight to the radius of the cylindrical melt (Preisser et al. 1983), and the shape of the melt often characterized with the volume ratio (Hu et al. 1994).

2.3.1. Onset mechanism

One of the first theoretical investigations in half-zone models were demonstrated by Neitzel *et al.* (1993) and Kuhlmann & Rath (1993). In both studies, the two-dimensional base state was computed numerically and for that the linear disturbance growth in three-dimensional system was computed.

The onset mechanism of the instability for a low Pr liquid was identified to be a purely hydrodynamic instability. Levenstam & Amberg (1995) carried out a numerical simulation for two low Pr liquids with Pr = 0 and 0.01. Since Ma_{cr} remained exactly the same for two cases, they concluded that the oscillation is caused by a hydrodynamical instability, similar to the one of a vortex ring. Further exploration of the dependence of the onset on Prwas performed using the linear stability analysis for a range of low and high Pr by Wanschura et al. (1995). For low Pr liquid flows, they drew similar conclusions to that of Levenstam & Amberg (1995). As for high Pr liquids, the instability was attributed to the heat transport coupled with the Marangoni effect, with a mechanism similar to the hydrothermal wave in shallow layers. In fact, there are certain correspondences between observations in half-zones and the hydrothermal wave, such as maximum disturbances in the interior and the oblique traveling waves. In the intermediate Pr regime (Pr = 0.07 -0.84), Levenstam et al. (2001) carried out numerical simulations and linear stability analysis which showed that the thermocapillary forces counteract the hydrodynamical instability, thus the axisymmetric base state is much more stable than for high or low Pr.

2.3.2. Supercritical oscillation

The bifurcation of the oscillation was shown to be supercritical in the experiment of Preisser et al. (1983), where they measured the amplitude of the oscillation for a range of supercritical Ma. This was followed by Velten et al. (1991) where the dominant wavenumber was checked for flows with strong nonlinearity raising the Ma up to a few times the critical value. Recently, more works have been reported to characterize the supercritical behavior of the oscillatory flow. In connection with the bifurcation theory, Leypoldt et al. (2000) have described the feature of the supercritical Hopf bifurcation by means of a numerical simulation.

Further increase in the temperature gradient will result in the transition to chaotic state. Ueno et al. (2003) has shown the change in the flow structure during the transition. Some interesting flow patterns were observed in the transitional regime by Schwabe et al. (1996) and Kawamura et al. (2002). Seeding the flow with particles, three-dimensional structures were revealed by particles accumulating along a single closed orbit.

2.4. Annular configuration

Another popular geometry to realize thermocapillary instabilities is the annular configuration. As shown in figure 2.3(c), the system is an open cylindrical container filled with a liquid to have a top free surface. The inner and outer cylinders are prescribed with different temperatures. Thermocapillary convection is thus driven by imposing a radial temperature gradient on the flat free surface. There are various types of annular configurations with differences in the ratio of the inner to outer radius, $H_r = R_h/R$, and the direction of the temperature gradient.

2.4.1. Small H_r

The classical setup is with $H_r \ll 1$ and negative temperature gradient along the radial axis, the geometry first suggested by Kamotani et al. (1991). The bottom temperature condition is adiabatic. Although the annular geometry does not reproduce the industrial applications layout, a generic flow of a character similar to that found for instance in the floating-zone method can be studied. The motivation is to acquire better quantitative data to gain more understanding of the mechanism of the thermocapillary instability. In half-zone model experiments, since the gravitational force deforms the liquid-gas interface, it is difficult to measure or maintain the shape of the interface. This is problematic for qualitative analysis and also comparison with numerical data. On the other hand, in annular configuration, having the free surface perpendicular to gravity, it can be kept flat, thus better quantitative analysis can be achieved.

Thus far, this type of annular flow has been studied only for high Pr fluids. The first demonstration of the thermocapillary oscillation was done by Kamotani $et\ al.\ (1991)$. A three-dimensional oscillatory flow with a periodic surface temperature pattern was observed. In a ground-based experiment, Kamotani $et\ al.\ (1996)$ measured critical temperature differences for various container size with the same H_r and $Pr\ (=27\ at\ 25^{o}C)$ and the upper limit of the container size below which the Marangoni convection dominates over the buoyancy convection was identified.

In a micro-gravity experiment, the cell can be enlarged to a significant extent. In 1992, the system was brought up to space to conduct a microgravity experiment (Kamotani et al. 1995). The steady thermocapillary flow was investigated and results were compared to a numerical study. In more recent microgravity experiments by Kamotani et al. (2000), the onset of the oscillation was investigated. Comparison between the data obtained in microgravity and the ones from normal gravity showed good agreement (Kamotani et al. 1996).

2.4.1.1. Onset mechanism

As discussed in Kamotani et al. (1999, 2000), they observed that Ma at the onset is not consistent for flows in annuli with different gap length, $R_g = R - R_h$ and constant height. With absence of gravitational effect, if only the thermoapillary convection plays a main role in the instability, one would expect the onset to be specified by certain value of Ma_{cr} . However, the experiments cited above showed an almost linear increase of Ma_{cr} with R_g . They attributed this behavior to free surface deformation at the hot corner region. A mechanism was proposed to be due to the surface deformation altering the surface velocity through a radial pressure gradient. Coupled with the thermocapillary heat transfer, this process is amplified. It was suggested that the onset of the oscillation depends on the ratio of the deformation to horizontal thermal boundary layer thickness, which was given the name S parameter. Computing S for the above flows with various R_g , consistent critical value of S was obtained. A similar argument was also made for the half-zone models by Masud et al. (1997).

Noting that the variation in R_g causes a change in the aspect ratio, it is not surprising that Ma_{cr} is not consistent since the linear stability characteristics will change. In this sense, introduction of S parameter is a challenging idea where a parameter independent of aspect ratio is searched for.

Despite of the demonstrations of the use of S parameter cited above, this scenario for the instability mechanism is not widely accepted yet. One reason is the magnitude of the surface deformation. As mentioned in Kamotani $et\ al.$ (2000), the deformation is very small; a few micro meters at the onset. This was comparable to the random surface deformation caused by the residual gravity, which seems not to alter the onset. It might be more natural to think that this minute surface deformation is a secondary response to the oscillation. Another reason is that there are some works reported to show reasonable comparisons between experiments and numerical simulations with non-deformable free surface for both the half-zone (Leypoldt $et\ al.$ 2000) and the annular configuration (Lavalley $et\ al.$ 2001).

2.4.2. Large H_r

Another type of annular configuration is with a large inner cylinder, $H_r \sim O(1)$. In the original setup of Schwabe *et al.* (1992), thermocapillary convection was driven outwards in a shallow liquid layer by heating the inner cylinder with respect to the outer cylinder. The bottom wall is connected to the cold outer wall. The aim of the experiment was to experimentally realize the hydrothermal wave predicted by Smith & Davis (1983). In order to satisfy the correspondence to the theory with infinite length in the spanwise direction, the annular gap was used. More recently, with similar geometries, both micro- and normal-gravity experiments was reported by Schwabe & Benz (2002). Here, the direction of the

temperature gradient is reversed by heating the outer wall instead. This was done to keep resemblance to the Czochralski crystal growth technique (Pfann 1966; Zief & Wilcox 1967). The experiment was equipped with a possibility to change the annular depth and, consequently, they identified hydrothermal waves for a shallow annulus and more complicated spatio-temporal structure for a deep one.

CHAPTER 3

Basic concepts

3.1. Governing equations

Taking only temperature dependence of the surface tension into account, the surface tension, σ , is considered as a linearly decreasing function of the temperature,

$$\sigma = \sigma_0 - \gamma (T - T_0), \tag{3.1}$$

where σ_0 denotes the surface tension at reference temperature T_0 . The surface tension coefficient, γ , has a positive value for most of the liquids, therefore the flow is driven against the temperature gradient on the free surface.

We assume the system to be an incompressible Newtonian flow. Therefore, the flow is governed by the incompressible Navier-Stokes equations, energy equation, and continuity equation. Here, the equations are shown for an annular geometry, though the difference is minor in the case of a half-zone. The coordinate system of the annular geometry is shown in figure 2.3(c). To simulate flows in axisymmetric geometries, the equations are expressed using the cylindrical coordinates as

$$\frac{\partial \mathbf{u}}{\partial t} + (\mathbf{u} \cdot \nabla)\mathbf{u} + \nabla p - \frac{Pr}{Ma} \nabla \cdot (\nabla \mathbf{u} + \nabla \mathbf{u}^{\mathrm{T}}) = \mathbf{0}, \tag{3.2}$$

$$\frac{\partial \theta}{\partial t} + (\mathbf{u} \cdot \nabla)\theta - \frac{1}{Ma} \nabla \cdot (\nabla \theta) = 0, \tag{3.3}$$

$$\nabla \cdot \mathbf{u} = 0, \tag{3.4}$$

where \mathbf{u} , θ and p are the velocity vector (u, v, w), temperature and pressure. These equations have been nondimensionalised using the length scale, R, temperature difference, ΔT , velocity scale,

$$U = \frac{\gamma \Delta T}{\mu} \tag{3.5}$$

and time scale,

$$t = \frac{R}{U},\tag{3.6}$$

where μ is the dynamic viscosity. The velocity scale U is derived by the balance between the radial surface tension gradient and the shear stress due to the normal velocity gradient as,

$$\mu \frac{\partial u}{\partial z} = \gamma \frac{\partial T}{\partial r}.$$
 (3.7)

Scaling both the normal and radial length with the common length R, the velocity scale U can be obtained as in equation 3.5. The nondimensional parameters appearing above are Ma and Pr defined as,

$$Ma = \frac{\gamma \Delta TR}{\mu \alpha},\tag{3.8}$$

$$Pr = \frac{\nu}{\alpha},\tag{3.9}$$

where α and ν are the thermal diffusivity and kinematic viscosity, respectively. The Reynolds number can be expressed by Ma and Pr as,

$$Re = \frac{Ma}{Pr} \tag{3.10}$$

In the annular configuration, the system is subjected to the boundary conditions,

$$\mathbf{u} = \mathbf{0}, \quad \theta = 1 \quad \text{at} \quad r = H_r,$$
 (3.11)

$$\mathbf{u} = \mathbf{0}, \quad \theta = 0 \quad \text{at} \quad r = 1, \tag{3.12}$$

$$\frac{\partial v}{\partial z} = \frac{\partial \theta}{\partial \phi}, \quad v = 0, \quad \frac{\partial u}{\partial z} = \frac{\partial \theta}{\partial r} \quad \text{at} \quad z = A_r,$$
 (3.13)

$$\mathbf{u} = \mathbf{0}, \quad \frac{\partial \theta}{\partial z} = 0 \quad \text{at} \quad z = 0,$$
 (3.14)

where $H_r = R_h/R$ and $A_r = H/R$.

Now, we consider the actuation of the system by heating and/or cooling the free surface. Assuming that the temperature modification is done purely by heat conduction on the liquid-gas interface, the control can be simulated by an additional boundary condition,

$$\frac{\partial \theta}{\partial z} = q(r, \phi) \quad \text{at} \quad z = A_r,$$
 (3.15)

where q is the nondimensional heat flux which represents the control perturbation.

3.2. Scaling analysis

In this section, some important scales are presented. We consider a stationary two-dimensional problem of equations (3.2) - (3.4). For convenience, the momentum equation (3.2) can be reformulated using a vorticity formulation,

$$Re\mathbf{u} \cdot \nabla \omega = \nabla^2 \omega \tag{3.16}$$

with corresponding changes in the boundary conditions, where ω is the vorticity.

The scaling is carried out assuming that the velocity and thermal length scales along the free surface can be characterized by a single length scale l. Here, the characteristic velocity scale along the surface is u_o and $\Delta T = O(1)$. Let δ and δ_T be the vertical length scales of the velocity shear and the thermal gradient at the free surface. Then we obtain

$$Re\frac{u_o}{l} \sim \frac{1}{l^2} + \frac{1}{\delta^2},\tag{3.17}$$

$$Ma\left(\frac{u_o}{l} + \frac{u_o\delta}{l\delta_T}\right) \sim \left(\frac{1}{l^2} + \frac{1}{\delta_T^2}\right).$$
 (3.18)

Now, we can derive a conventional scale, the ratio of the velocity to thermal boundary layer thickness as,

$$\frac{\delta}{\delta_T} = Pr^{1/2}. (3.19)$$

In addition, the thermocapillary boundary condition is scaled as,

$$\frac{u_o}{\delta} \sim \frac{1}{I}.\tag{3.20}$$

When $Pr \ll 1$, since the temperature field is determined mostly by conduction, rather straightforward scaling can be carried out. Here the thermal boundary layer will be absent $(\delta_T \sim 1)$ and surface temperature has a monotonous profile $(l \sim 1)$. The simplest case is when the flow is dominated by the viscous force $(Re \ll 1)$, then all the scales used for non-dimensionalization are correct $(u_o \sim \delta \sim 1)$. For the conductive and inertial flow within the limit of $Pr \ll 1$ and $Re \to \infty$, we obtain, from equations (3.17) and (3.18),

$$\delta \sim Re^{-1/3},\tag{3.21}$$

and from scaling of the continuity equation,

$$u_o \sim Re^{-1/3}$$
. (3.22)

Hence the effective Reynold's number, Re_{eff} , is

$$Re_{eff} \sim Re^{2/3}. (3.23)$$

3.2.2. *High Pr*

The problem is more complicated for high Pr liquids since the isotherms are distorted by the convection. Attention has been paid to different regions in the geometry, the hot/cold corner region near the contact of the hot/cold wall and the free surface, and the bulk flow which is the rest of the geometry. Giving separate attention to those regions, some scales have been identified. The scaling of the viscous flow ($Re \sim O(1)$) in the hot corner region was studied by Cowley & Davis (1983). By assuming an insulated vertical wall to obtain the scales in the boundary layers along the vertical wall, and scaling the surface boundary layers with thermocapillary balance together with global heat conservation, the following scaling can be derived,

$$u_{core} \sim Ma^{1/7}, \ \Delta_h \sim Ma^{-2/7}, \ \delta_h \sim Ma^{-3/7}, \ Nu \sim Ma^{2/7},$$
 (3.24)

where u_{core} and Δ_h are the velocity in the core far away from the boundaries and the viscous boundary thickness along the hot wall. Nu is the Nusselt number on the hot wall. The notations are described in figure 3.1. The subscript h and c denotes the values in the hot and cold regions.

For the cold corner region, Canright (1994) clarified the various scalings for different characteristics of the flow (Pr, Ma) including the ones for convective and viscous states,

$$u_o \sim 1, \ l_c \sim Ma^{-1}, \ \delta_c \sim Ma^{-1}.$$
 (3.25)

For thermocapillary flows in closed geometries, such as the half-zone and the annular configuration, the scaling laws (3.21) and (3.22) are probably the most important ones. Although, in a strict sense, these scaling laws are limited to conductive and inertial flow, even for high Pr inertial flow, the scalings are not far off and are useful to grasp the scales of the characteristic physical quantities. In convective and inertial flow, the cold corner region is pressed towards the cold wall and, consequently, the length scale l_c becomes very small. Since the surface temperature in the rest of the region decreases outwards rather gradually, in a rough sense, $l \sim R$. The above discussion would become less accurate as Ma increases to form a plateau in the surface temperature profile around the mid-gap since then the length scale l becomes smaller than R.

Recently, some works were reported on the scaling of the specific closed-geometry problems. Here, the scales for inertial flows would be of particular interest. The base flows of the half-zone and annular configuration show different characteristics due to the difference in the flow fields on the free surface. In an annular flow, unlike in the half-zone, the flow diverges on the free surface. As a consequence, for a half-zone inertial flow, the core of the convection is located close to the hot corner, whereas in annular flow, the core is located rather closer to the cold wall. This gives rise to the different thicknesses or vertical scales in the velocity boundary layer.

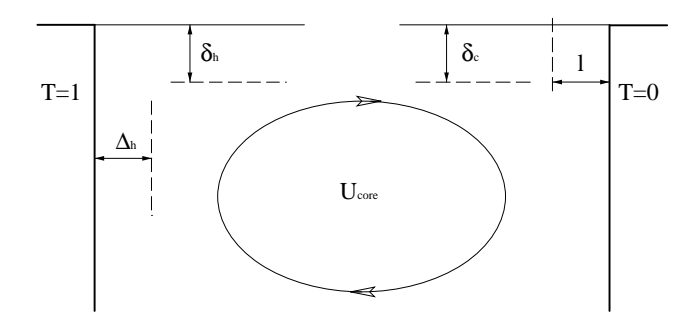


FIGURE 3.1. Sketch of the geometry together with the notations introduced in the scaling analysis (Kuhlmann 1998).

Kamotani & Ostrach (1998) and Kamotani et al. (2000) describe the above differences by suggesting that in overall, the flow is mainly driven in the hot corner for the half-zone and in the bulk region for the annular configuration. They defined a length scale Δ , the distance from the hot corner to the velocity peak on the free surface, and considered the thermocapillary stress balance in the region. Observing constant velocity and temperature gradient in this region, they assumed that the free surface flow is purely conductive, and therefore the convection in the thermal boundary layer along the hot wall is balanced by the conduction in the hot corner. Furthermore, the average velocity along the hot wall should scale with u_o . Together with the balance between convection and conduction in the thermal boundary layer along the wall and global heat conservation, the following scales were derived;

$$u_o \sim Ma^{-1/7}, \ \Delta \sim Ma^{-1/2}, \ Nu \sim Ma^{2/7}.$$
 (3.26)

For the annular configuration, they suggested to base the scaling on the bulk flow characteristics. Based on the observation that the vertical location of the vortex core has weak dependence on Ma, the bulk flow was assumed to be viscous dominated. The velocity can be determined by balancing the shear stress with the surface tension gradient due to the characteristic temperature variation in the bulk region. By considering the scaling for continuity and heat transport in the bulk region together with the global heat conservation, they derived,

$$u_o \sim u_{core} \sim Ma^{-1/5}, \ \delta \sim Ma^{-2/5}, \ Nu \sim Ma^{1/5}.$$
 (3.27)

3.3. Modal structures

In axisymmetric flows, the thermocapillary instability arises with a distinct azimuthal wavenumber. The selection of the most dangerous mode depends strongly on the geometrical parameters such as the aspect ratio and also, in case of an annular configuration, the ratio of inner to outer radius. In the half-zone models with Pr = 7 liquid, Preisser *et al.* (1983) experimentally found that the dominant wavenumber n can be related to the aspect ratio as,

$$nA_r = c, (3.28)$$

where $c \sim 1.1$. This was later confirmed in the numerical simulation of Leypoldt et~al.~(2000), where they computed the constant $c \sim 1.2$. The Pr dependence of the relation (3.28) is yet not clear. For high Pr, Ueno et~al.~(2003) carried out experiments with various liquids with high Pr~(=14,28,68) and observed a weak dependence of the wavenumber on Pr. On the other hand, for low Pr liquids, ideas have been presented based on analogies with the vortex ring instability (Levenstam & Amberg 1995) and the transient flow structure in Poiseuille flow (Wanschura et~al.~1995). However, at this stage, these analogies are no more than speculations, and more studies would be needed. In the annular configuration, to this date, there is no reported work on the selection of the azimuthal wavenumber. The difficulty lies in the complication due to an additional geometrical parameter, H_r , the ratio of inner to outer radius.

It is interesting to know if the dominance of the onset mode structure remains the same in the regime with stronger nonlinearity. The wave structure for a range of supercritical Ma is visualized in the experiment of Ueno $et\ al.$ (2003). They presented a case where the wavenumber of the fundamental mode remained visible to about three times Ma_{cr} . Above that value of Ma, the chaotic signals were observed in local temperature measurements. In this regime, the mixing of the tracer particles is too strong to allow examination of the flow structure with flow visualization. In this context, an interesting feature of a low Pr system is reported by Sumiji $et\ al.$ (2002) where they measured surface temperature fluctuations in a silicon melt at two azimuthal locations by a non-intrusive method. Chaotic temporal signals were observed, however, the correlation of the signals from different sensors indicated that the spatial modal structure was still preserved.

3.3.1. Traveling or Standing?

In one of the first temperature measurement of the oscillatory flow with multiple sensors, Velten et al. (1991) observed that signals at all three sensors were in phase, which they originally suggested to be due to the axisymmetric oscillation. Later, it was revealed with help from flow visualization techniques that the oscillation can take a form of a standing wave. There is still ongoing discussion on if the onset wave structure is standing or traveling. Many reported works carried out with different fluids and geometries do not seem to reach a consensus.

In a half-zone model, Savino & Monti (1996) showed, performing a numerical simulation for Pr = 30 and $A_r = 0.5, 1$, that the instability arises as a standing wave at the onset of the oscillation due the symmetry of the problem

but when a fully established periodic state is reached, the solution will be a traveling wave. The aspect ratio, A_r , is defined as the ratio of the hight to radius of the liquid bridge. They mention that their results are in agreement with the micro-gravity experiment of Monti et al. (1994). For Pr=4 and 7 and a wide range of A_r from 0.5 to 1.3, Leypoldt et al. (2000) also reported that the traveling wave is the only stable solution. On the other hand, Ueno et al. (2003) performed experiments varying the viscosity of Silicone oil, $\nu=1-5$ cSt, and the aspect ratio, $A_r=0.3-2.0$, and found that the onset structure of the oscillation was standing.

In an annular configuration, Kamotani et al. (2000) observed, using a fluid with $\nu=2$ cSt in the micro-gravity experiments for a range of aspect ratios, that the oscillation is traveling at the onset and becomes standing as Ma increases. The same trend has been observed by Sim & Zebib (2002) in a numerical simulation for Pr=17. On the contrary, Lavalley et al. (2001) showed in their numerical simulation that the onset oscillation is standing and becomes traveling as Ma increases. Carrying out an experiment with the same geometry as Lavalley et al. (2001), we observed only traveling waves for a range of Ma with some uncertainty on judging the structure close to the onset (Paper 2).

At this stage, nothing conclusive can be said on what triggers different structures. We can only raise the possible causes that might make the difference such as the aspect ratio, volume ratio, heat conduction through the free surface, Pr, and grid resolution in case of numerical simulations.

3.4. Weakly nonlinear analysis

In order to analyze the weakly nonlinear state close to the onset of the instability, formulation of amplitude equations is useful. The derivation of amplitude equations for the classical Marangoni convection was carried out by Rosenblat et al. (1982a,b). They considered eigenfunction expansions based on the eigenfunctions of the linear stability problem and adopted the Galerkin procedure. Consequently, they obtained the equation from the amplitude of the dominant mode (A),

$$\frac{\partial A}{\partial t} = c_1 \epsilon A - c_2 A^3, \tag{3.29}$$

where the values of the coefficients c_1 and c_2 depend on the given problem with various geometrical parameters. ϵ is the overcritical parameter defined as

$$\epsilon = \frac{Ma - Ma_{cr}}{Ma_{cr}}. (3.30)$$

For the thermocapillary oscillation in the system with a temperature gradient parallel to the surface, the weakly nonlinear analysis has been performed only for hydrothermal waves in a shallow liquid layer by Smith (1988), where finite amplitudes of the modal structures close to the criticality are derived.

With the standard asymptotic expansion with multiple scales, the amplitude equations for left and right traveling waves were derived to take the general form of the celebrated Ginzburg-Landau equation.

Such a formulation of the amplitude equation for the thermocapillary instability of axisymmetric base flow would be difficult, at least analytically, and hence it is not available to this date. However, distinct evidence concerning the bifurcation characteristics, as shown in section 3.5, suggests that the amplitude equation of the oscillation may a from similar to equation (3.29).

Recently, for a half-zone flow, Leypoldt et al. (2000) characterized the temporal evolution of the complex amplitudes of the two traveling waves with opposite directions of azimuthal propagation by basing their analysis on the Ginzburg-Landau equation. A temporally and spatially periodic wave can be described as the sum of clockwise- and counterclockwise-travelling waves with amplitudes A_+ and A_- . If the state is translation-invariant in the wave (azimuthal) direction, fluctuations of the temperature and velocities, $\mathbf{s} = (\theta', \mathbf{u}')$, can be expressed as,

$$\mathbf{s}(r,\phi,z,t) = \mathbf{s}_o(r,z)[A_+(\phi,t)e^{in\phi} + A_-(\phi,t)e^{-in\phi}]e^{-i\omega t} + c.c., \tag{3.31}$$

where \mathbf{s}_o is the eigenvectors of the linear stability problem and ω is the critical angular frequency (Cross 1988). In the weakly nonlinear limit, the slow temporal and spatial modulations resulting from the weak nonlinear coupling can be captured by the slow variation of the complex amplitudes A_+ and A_- . In this limit, considering a one dimensional problem in ϕ , the amplitude equations take the form of general Ginzburg-Landau equations,

$$\tau_{o}(\frac{\partial}{\partial t} + v\frac{\partial}{\partial x})A_{+} = \epsilon(1 + ic_{o})A_{+} + (1 + ic_{1})\xi_{o}^{2}\frac{\partial^{2}A_{+}}{\partial x^{2}} -g_{1}(1 + ic_{2})|A_{+}^{2}|A_{+} + g_{2}(1 + ic_{3})|A_{-}^{2}|A_{+},$$
(3.32)

$$\tau_{o}(\frac{\partial}{\partial t} + v \frac{\partial}{\partial x}) A_{-} = \epsilon (1 + ic_{o}) A_{-} + (1 + ic_{1}) \xi_{o}^{2} \frac{\partial^{2} A_{-}}{\partial x^{2}} -g_{1}(1 + ic_{2}) |A_{-}^{2}| A_{-} + g_{2}(1 + ic_{3}) |A_{+}^{2}| A_{-},$$
(3.33)

where v is the group velocity and $\tau_o, g_1, g_2, c_o, c_1, c_2, c_3$ are real coefficients. Since the thermocapillary wave with order of unity aspect ratio exhibits a certain integer wavenumber, we disregard the slow spatial-amplitude modulations. Then the equations for the real amplitudes \hat{A}_+ and \hat{A}_- can be calculated to be,

$$\tau_o \frac{\partial \hat{A}_+}{\partial t} = \epsilon \hat{A}_+ - g_1 \hat{A}_+^3 - g_2 \hat{A}_-^2 \hat{A}_+, \tag{3.34}$$

$$\tau_o \frac{\partial \hat{A}_-}{\partial t} = \epsilon \hat{A}_- - g_1 \hat{A}_-^3 - g_2 \hat{A}_+^2 \hat{A}_-. \tag{3.35}$$

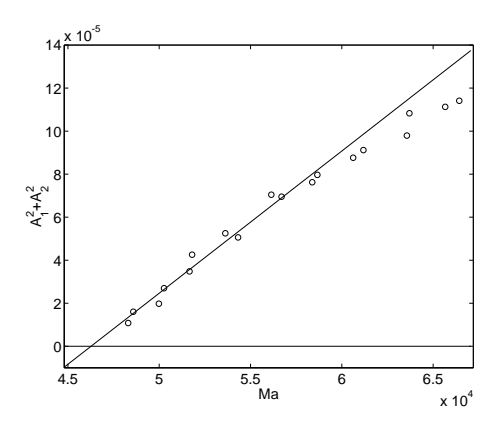


FIGURE 3.2. Bifurcation curve of the uncontrolled thermocapillary oscillation in an annular flow. Circles: The amplitude of the oscillation. Line: The square root curve fit to the data. Extrapolating the line to $A_1^2 + A_2^2 = 0$, we obtained the critical Marangoni number $Ma_{cr} = 46270$.

Now, considering the pure traveling wave with $A_{-}=0$, the equations are reduced to the same form as equation (3.29).

3.5. Bifurcation theory

The amplitude equation (3.29) takes the form of a classical example in bifurcation theory (Iooss & Joseph 1989; Strogatz 1994). Depending on the sign of the coefficients, the system can exhibit different types of bifurcation characteristics. On fixing c_1 to have a positive value, the oscillation exhibits the supercritical and subcritical Hopf bifurcation for positive and negative c_2 , respectively. As for the thermocapillary waves in axisymmetric base flow, the bifurcation is detected to be supercritical without any hysteresis with change in ϵ . In case of supercritical Hopf bifurcation, the amplitude grows continuously from zero and increases proportionally to $\sqrt{\epsilon}$. This general feature was observed in both half-zone models (Leypoldt *et al.* 2000, Paper 3) and annular configurations (Lavalley *et al.* 2001, Paper 2) by means of numerical simulations and experiments. The experimental result from Paper 2 is shown in figure 3.2.

Now we consider a possibility to alter the coefficients such that

$$\dot{A} = (c_1 \epsilon - G_1)A - (c_2 + G_3)A^3, \tag{3.36}$$

where G_1 and G_3 are positive constants. Naturally, variation of G_1 can alter the linear term, i.e. criticality of the oscillation. When $c_2 < G_3$, the bifurcation is supercritical and the slope of the bifurcation curve decreases with G_3 . Therefore, if there are accessible means to alter these coefficients, it would be possible to change the bifurcation characteristics in a favorable way. Generally, in industrial applications, the supercritical bifurcation is preferred to the subcritical one since the latter is accompanied with a sudden appearance of the oscillation with a finite amplitude on crossing the criticality. In a thermal convection loop problem, which is the experimental realization of the celebrated Lorenz equations, the original subcritical Hopf bifurcation which leads the state to a chaotic one, was changed to supercritical bifurcation using a cubic control by Yuen & Bau (1996).

3.6. Routes to chaos

Studies in nonlinear dynamics and chaos have revealed that the chaotic state can be reached through different scenarios such as period-doubling, quasiperiodicity and intermittency (Strogatz 1994). In the period-doubling scenario, increasing the experimental parameter, λ (Ma in the current problem), the period of the oscillation changes to approximately double the period of the original one. One of the most interesting features of this scenario is that critical values of λ for the *i*th period doubling, λ_i , satisfies the quantitative universality discovered by Feigenbaum (1978, 1979),

$$\frac{\lambda_i - \lambda_{i-1}}{\lambda_{i+1} - \lambda_i} = 4.669\dots$$
 (3.37)

Although this originated in analyses of simple mathematical systems, the law was later confirmed in experiments by Libchaber *et al.* (1982) for the natural convection of liquid mercury in a box container heated from below. To this date, the period-doubling scenario has been observed in a number of physical systems including hydrodynamical problems such as the Taylor vortex flow (Wiener *et al.* 1997).

An evidence is presented in Paper 3 which shows that the transition to chaotic state in a high Pr half-zone flow, can follow a period-doubling scenario. From the temperature signal measured on the free-surface, a three-dimensional return map can be constructed as shown in figure 3.3 (a). The map shows that the oscillation is in a state of period-doubling with period-4 cycle, the beginning of a cascade which leads the system to chaos. Although no detailed analysis was performed to verify the quantitative feature of the period-doubling, from rough observations of the delay maps for different Ma, the transition did not seem to follow the quantitative universality. However, this could be due to the fact that the experiment is far from a single parameter problem in this range of high Ma, and hence a better controlled experiment could be of interest to explore the period-doubling characteristics.

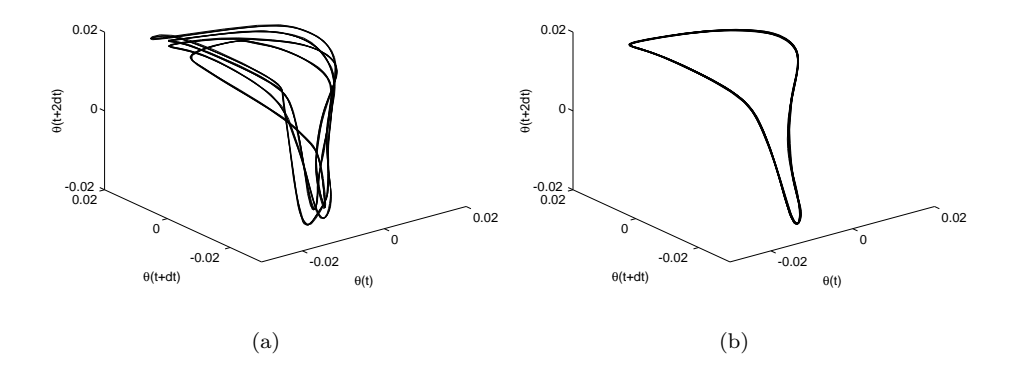


FIGURE 3.3. Three-dimensional return maps of a temperature oscillation in the period-doubling regime. (a): Uncontrolled state, (b): Subjected to a linear control.

CHAPTER 4

Active control of thermal convection

4.1. Control of natural convection

For industrial applications, it is beneficial to control convective flows to achieve the preferable flow characteristics. In many situations, the goal is set to delay the transition of instabilities or to attenuate the supercritical disturbances. Taking material science applications into account, a classical key target of control is the natural convection driven by the buoyancy force. When the flow has a well defined spatial wavenumber, the system can be controllable with a limited number of sensors and actuators, thus feedback control can be applied more easily.

Between internal and external natural convection, the former natural convection has caught more recent attention as the target of control since the closed geometry makes the feedback control possible. Some cases of successful control have been reported for flows in various geometries with different ways of imposing temperature gradients. Many of the works have been carried out by the group of Bau, the pioneers in this field of study. Their methodology is to first have a set of simple model equations available, then carry out stability analysis as well as numerical simulations to check the performance of the control in terms of the stability limit and bifurcation analysis. The results are finally validated by experiments.

There is still a large distance between the numerical studies adopting sophisticated control schemes such as the optimal control scheme and experimental studies where application of such control schemes face serious difficulties because of not only the lack of experimental tools, but also the heavy real-time computation it would require. Being a slow phenomenon with limited number of modes playing a role in the instability, the study of the thermal convection could be the bridge between the two stances. Also, being a classical problem which has been intensively studied, some promising simplified model equations are available for pre-testing the control performance and identifying the system in real-time.

One of the first works to utilize feedback control to stabilize thermal convection was carried out by Wang *et al.* (1992) who applied proportional control in a thermal convection loop, and managed to suppress the chaotic behavior.

Later, Yuen & Bau (1996) succeeded to change a subcritical Hopf bifurcation to a supercritical one using cubic control. An attractive feature of this problem is that the system can be well described by a set of model equations which are essentially the celebrated Lorenz's equations. Based on the model equations, theoretical and numerical analyses were carried out together with experiments.

Using a similar methodology, these works were followed by the series of works on Rayleigh-Bénard convection. For two-dimensional Rayleigh-Bénard convection, Tang & Bau (1993) theoretically demonstrated the possibility to delay the onset of the convection by almost one order of magnitude. This was followed by the experimental work of Howle (1997) where feedback control realized significant suppression of two-dimensional convection in a slender box. The control method was also tested for three-dimensional convection by Tang & Bau (1998), but the obtained stabilization fell short of the theoretical prediction done for two-dimensional convection.

Recently, a few theoretical works have been reported on feedback control of the transition from no-motion state to time-independent motion in Marangoni-Bénard convection. Linear control was applied to delay the onset of the instability by Bau (1999). The delay of transition was confirmed by means of linear stability analysis. Or et al. (1999) demonstrated the possibility of controlling the long wavelength mode by a weakly nonlinear control law. Nonlinear flow properties could be altered to eliminate the subcritical nature of the bifurcation. A similar analysis was applied to the finite wavelength mode by Or & Kelly (2001), taking the buoyancy effect into account.

4.2. Control of steady thermocapillary convection

4.2.1. Base flow control

The simplest way to delay the onset of the oscillation would be to weaken the base flow. If the purpose is only to suppress the Marangoni convection, some of the suggested contacting methods such as partially covering (Lan & Kou 1991a,b) or coating (Eyer & Leiste 1985) the free surface of the melt would be most efficient. However, since that would cause a contamination and dull the original merit of the floating-zone technique, a contact-less method is preferred.

A well known method to attenuate the fluctuations in the electronically conductive melt is to apply a magnetic field to the melt-zone. The magnetic field has an effect to weaken the axisymmertic base convection, in other words, to decrease the effective Ma, and thus the fluctuation is attenuated. One of the first works of this kind was reported by Leon et al. (1981) where an axial magnetic field was applied in a float-zone of high-resistivity silicon. This was followed by a series of experimental observations by applying both transverse (Kimura et al. 1983; G. D. Robertson & O'Connor 1986b) and axial (G. D. Robertson & O'Connor 1986a) magnetic field, where the efficiency of the axial magnetic field was found to be superior to the transverse one. Dold

et al. (1998) applied a weak static axial magnetic field and found that although the reduction of the fluctuation can be achieved, the magnetic field causes a separation of the flow field in a quiescent center periphery mixed by thermocapillary convection, which gives rise to the deterioration of the radial homogeneity. Although this could be remedied by strengthening the magnetic field, that would lead to the appearance of another type of strictions due to thermoelectromagnetic convection caused by the interaction of thermoelectric currents with the magnetic field (Cröll et al. 1998). The appearance of the thermoelectromagnetic convection can bring a tremendous complexity to the analysis and application of the method due to the difficulties in prediction and control of the convection. In some of the recent studies, a rotation is added to the system in order to improve the method with a weak magnetic field. The method was shown to reduce the fluctuation while the radial homogeneity was maintained (Fischer et al. 1999; Dold et al. 2001). The efficiency of the control increases with the length of the melt diameter, however, remaining dopant striations with smaller intensity and higher frequency than the original ones were still observed in the balanced state. The possibility for the rotating magnetic field to induce Taylor vortices is discussed by Kaiser & Benz (1998).

A method to directly counteract the thermocapillary flow was first suggested by Dressler & Sivakumaran (1988), where they attempted to counteract the steady thermocapillary flow by directing a gas jet parallel to the surface. Later, Anilkumar et al. (1993) suggested the idea to generate a surface stream flow by vibrating the solid end of the liquid bridge and oppose the steady thermocapillary flow on the surface. In these first works, the possibility to generate a streaming strong enough to balance the thermocapillary flow is shown in a half-zone using Silicon oils with high viscosities up to 100 cSt. Following these first demonstrations, the method was applied to suppress thermocapillary convection in a sodium nitrate melt (Shen et al. 1996). In floating-zone configurations, between the two half zones appearing on top of each other, the target of the control would be the vortex close to the freezing interface which plays an important role for the solidification process. Consequently, promotion of microstructual homogeneity could be observed in the re-solidified materials. One of the difficulties in this method is that the strength of the streaming for a certain end-wall vibration decreases with the viscosity. Thus far, this fact is preventing this method to be applied to low viscosity melts such as silicon. In terms of the flow physics, despite of recent theoretical and numerical works (Lee et al. 1996; Lee 1998), the three dimensional interaction between the streaming and steady thermocapillary convection is yet not clear.

Another way to reduce the base flow was recently suggested in Azumi et al. (2001) where the basic convection velocity in a silicon melt could be reduced by altering the partial pressure of the oxygen. Since the magnitude of the surface tension coefficient of the melted silicon decreases with the oxygen partial pressure, increasing pressure leads to decrease in the surface tension

gradient, and hence the driving force can be weakened. Consequently they have observed a change from a complex oscillation with broad spectra to a single mode oscillation.

4.2.2. Control of thermocapillary instability

A drawback of the above mentioned methods to attenuate the fluctuation by reducing the steady convection is that the damping of the base flow enhances the macro-segregation of the chemical compositions due to the weakening of the mixing. Furthermore, in most of these methods, there is a difficulty in prediction, analysis and control of the three-dimensional dynamical interaction of the actuation and the state. Hence, it would be beneficial to investigate the possibility to suppress only the oscillation without altering the base state appreciably. Since the convective heat transport plays a key role in the thermocapillary instability, it should be possible to alter the stability characteristics by slightly modifying the temperature field. In addition, the temperature modification can be realized by heating/cooling on the free surface with a well-understood physical description, which should help us to examine the influence of the control to the flow. The idea is encouraged by the literature on natural convection control cited earlier, where this type of control using weak modification of the boundary temperature has been carried out.

With better understanding of the phenomena from extensive studies on the onset mechanism and nonlinear features of the instability, a few works have been reported on control of oscillatory thermocapillary convection in various geometries. An attempt to stabilize the thermocapillary wave instability in an experiment on a plane fluid layer was made by Benz et al. (1998). The temperature signal and phase information sensed by thermocouples near the cold end of the layer was fed forward to control a laser which heated the downstream fluid surface along a line.

For a half-zone model, Petrov et al. (1996, 1998) attempted to stabilize the oscillation by applying a nonlinear control algorithm using local temperature measurements close to the free surface and modifying the temperature at different local locations with Peltier devices. The control scheme inherits the idea of Ott et al. (1990). They have constructed a look-up table based on the system's response to a sequence of random perturbations. A linear control law using appropriate data sets from the look-up table was computed. The control law was updated at every time step to adapt the control law to the nonlinear system. Using one sensor/actuator pair, successful control was observed at the sensor location for $Ma \sim 17750$. However infrared visualization revealed the presence of standing waves with nodes at the feedback element and the sensor. This was resolved by adding a second sensor/actuator pair which enables the control to damp out both waves propagating clockwise and counterclockwise, thus standing waves. The performance of the control was reported for only one value of $Ma \sim 15000$, where the critical value was $Ma_{cr} \sim 14000$. They stated

that the oscillation could not be suppressed when Ma exceeds the critical value by more than 8.5%, mostly due to the weak response of the fluid flow to the Peltier devices, which cannot be cooled more than a few degrees during the application of the control pulse.

CHAPTER 5

Methodologies

5.1. Opposition control

In the present thesis work, the intention is to control oscillatory thermocapillary convection in axisymmetric geometries using an active feedback control scheme. The control is based on a simple linear feedback control law with sensors and actuators strategically positioned based on knowledge of the dominant azimuthal mode which is determined by the geometry of the system.

5.1.1. Proportional control

The linear feedback control law can be written as,

$$Q(\phi_i + d\phi) = G_1 \theta'(\phi_i), \tag{5.1}$$

where ϕ_i is the *i*th azimuthal sensor location and $d\phi$ is the distance between sensors and paired actuators. Q, G_1 and θ' are the actuator power output, linear control gain and non-dimensional temperature disturbance. The value of $d\phi$ can be varied according to various positioning of the controllers depending on the experimental feasibility, but should be

$$d\phi = \begin{cases} \frac{2j\pi}{n} - \frac{\pi}{n}, & G_1 > 0, \\ \frac{2j\pi}{n}, & G_1 < 0, \end{cases}$$
 (5.2)

where j is a positive integer. This way, a simple opposition control can be realized.

In the experiments, since we adopt heaters as actuators, the actuation is limited to heating only. Therefore, the actual output can be expressed, assuming point heat sources, as

$$Q(\phi_i + d\phi) = \begin{cases} G_1 \theta'(\phi_i), & G_1 \theta'(\phi_i) \ge 0\\ 0, & G_1 \theta'(\phi_i) < 0. \end{cases}$$
 (5.3)

5.2. Weakly nonlinear control

The cubic terms are added to the control law to apply a weakly nonlinear control. For instance, when the control gains have positive values, the control

law can be written as

$$Q(\phi_i + d\phi) = \begin{cases} G_1 \theta'(\phi_i) + G_3 \theta'(\phi_i) (\theta'(\phi_1)^2 + \theta'(\phi_2)^2), & \theta'(\phi_i) \ge 0\\ 0, & \theta'(\phi_i) < 0. \end{cases}$$
(5.4)

where G_3 is the cubic control gain. As discussed in section (3.5), a cubic control is often applied to change the bifurcation characteristics. Specifically, if the system shows a subcritical bifurcation, modification of the nonlinear properties of the system may render it to supercritical which is more easily controlled (Yuen & Bau 1996). Another merit is to modify the state without altering the criticality. As a consequence, we have taken advantage of the latter one.

5.3. Experiments

The above control method was experimentally applied to the two different geometrical models, the annular configuration and the half-zone. This topic covers the major part of this thesis. The task here is first to check the practicability of such a method, then to carry out quantitative analyses varying the parameters to verify its performance and limitations. The influence of the local feedback control can be examined in connection with the fundamental bifurcation theory. The explored parameter space consists of Ma, G_1 , G_3 and the selection of the sensor/heater positions. In this section, some of the key issues in the experiments are discussed.

In ground based experiments, the flow can be severely influenced by the gravitational force. When exploring the mechanism of the thermocapillary instability, one would prefer to establish a flow driven purely by the thermocapillary force. Furthermore, in order to simulate the material processing in space, the reduction of the gravitational effect is necessary. This can be done by reducing the size of the geometry. The criterion for the dominant thermocapillary convection can be expressed by considering the ratio between the buoyancy forces to thermocapillary forces as,

$$\frac{Gr}{Re_{eff}^2} = \frac{Gr}{Re^{4/3}} = \frac{Bo_d}{Re^{1/3}} < 1. \tag{5.5}$$

Here, the dynamic Bond number is $Bo_d = Gr/Re = \rho g \beta R^2/\gamma$, where ρ , g and β are the density, acceleration of gravity and thermal expansion coefficient. Gr is the Grashof number. For an annular geometry, Kamotani et~al. (1996) measured critical temperature differences for various container sizes with the same H_r and Pr(=27). The upper limit of the container size below which Marangoni convection dominates over buoyancy convection was identified. From the identified limit and other presented parameters, we can derive the criterion for negligible buoyancy effect, $Bo_d \leq 0.24$. In the annular configuration presented in this thesis, $Bo_d \leq 0.089$, hence we conclude that the buoyancy should be of

minor importance. Following this criterion, the gound-based experiment of this kind is compelled to keep the cell size to the order of millimeters. In addition to the difficulties in handling the instruments, one of the problems in measurement of physical properties in a small volume is the low signal to noise ratio. Especially, in the supercritical regime close to the onset of the instability, the magnitude of the oscillation could be relatively too small to be detected.

5.3.2. Temperature measurements

Many reported experimental works to determine the onset of the instability have encountered difficulties in the quantitative accuracy of measuring the amplitude of the oscillations. When the surface temperature is to be measured, the measurements were commonly made by contact-less techniques such as thermographs or placing thermocouples close to the free surface of the liquid.

An alternative way is to dip the thermocouples into the liquid, which may contaminate the flow field because thermocouples are rather large, especially for ground-based experiments where the system is made small to let the thermocapillary force dominate over the buoyancy force. When the relatively large object is installed through the free surface, influence of the developed meniscus could be significant. This is problematic, since the quantitative temperature measurement of the oscillation close to criticality would be very useful to determine Ma_{cr} .

Probably, at least in the ground-based experiments, the best method so far is to install the classical cold wire sensor through the free surface. The wire can be manufactured to have a shape of U, and dipped into the liquid until the bottom reaches a certain depth. Since the wire is typically a few microns thick, it can be installed through the free surface without causing any appreciable free-surface deformation. One of the difficulties in this method is the measurement sensitivity to the depth of the sensor installation. Since, close to the surface, the thermal boundary layer can be quite thin, the steep temperature gradient enhances the dislocation sensitivity. Another source of error could be the inevitable interaction between the sensor support and the thermal boundary layer in the gas. Nevertheless, with this method some convincing qualitative results were obtained. As shown in figure 3.2, a Hopf bifurcation curve could be measured successfully (Paper 2).

5.3.3. Actuation

As far as experiments are concerned, actuation plays the key role in active flow control problems. Especially, if one would like to connect the obtained control performance to physical interpretations or theoretical understandings, it is important to know how the flow is actually actuated. Many of the reported works in active flow control seem to struggle to manage the actuation to be describable in terms of mathematical formulation, especially when the velocity vector is to be modified. Compared with those cases, the fact that the flow can be altered by temperature modification can simplify the problem to a large extent.

To attenuate temperature fluctuations, the preferable function of the actuator would be to cool and heat alternately. This can be realized by using Peltier devices (Petrov et al. 1996) which heat or cool depending on the direction of the applied current. The problem with a Peltier device is that in order to keep up with the time response of the oscillation, the magnitude of the power output faces a severe limitation, which is not enough to explore the possibility to suppress oscillation in a range of supercritical Ma. Therefore, in the series of experiments presented in this thesis, the actuator is an heater. In this case, too, the time response of the temperature change in the heater is an issue. The heat conduction time scale of the heater needs to be less than the convective time scale of the oscillation. For this purpose, the heater was made to have a very small volume.

5.3.4. Liquid-gas boundary

In half-zone models, especially in the ones with large aspect ratios, the surface is inevitably deformed due to the gravity force as sketched in figure 2.3(b). To carry out quantitative analysis on control performance, it is important to prevent the surface shape from changing due to evaporation, since this may affect the stability properties as shown by Hu *et al.* (1994).

It is observed that the forced and natural convection formed in the gas layer could have significant influence on the liquid flow. In our half-zone experiment, though it is not presented in the thesis, we have observed in a regime very close the the criticality, that placing an object with low heat conductivity in the gas thermal boundary layer can strongly alter the flow.

5.3.5. Visualization techniques

In half-zone experiments, top-view flow visualization allows us to observe the mode structure in the $r-\phi$ plane as shown in figure 5.1(a–c). Here, a mode-2 standing oscillation is shown by a sequence of pictures. In this visualization technique, the modal structures are visualized as polygonal particle-free areas appears at the center of the plane. The number of lines of symmetry in the visualized image indicates certain polygonal modal flow structures. The polygonal particle-free area indicates the radial deformation of the vortical structure from the axisymmetric state. For $A_r=1$, the particle-free area appears to be an ellipse. Here, the number of lines of symmetry is 2 thus the oscillation has azimuthal wave number of 2 (mode-2).

The above visualization method is not applicable for annular flows because of the absence of such a particle-free zone indicating the modal structures. A common and most useful way to detect the wave structure for this geometry

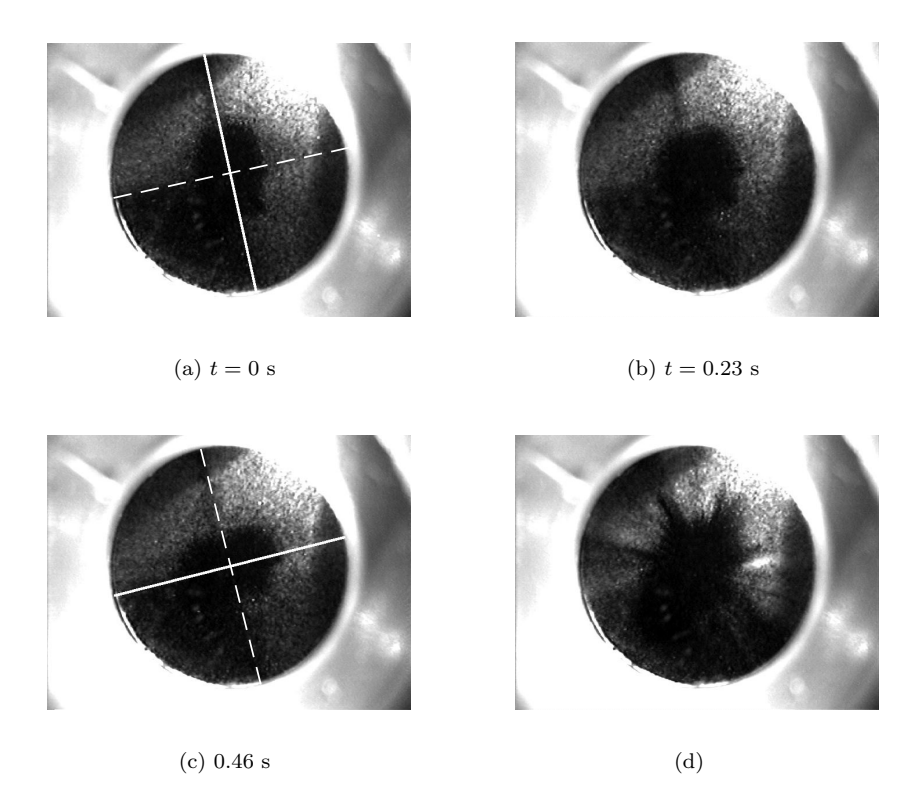


FIGURE 5.1. Flow visualization of a mode-2 standing wave. (a–c): Without control. (d): Time independent state achieved by proportional control. The solid and dashed lines represent the lines of symmetry. $\epsilon=0.18$.

is therefore to use thermography technique. An alternative is to visualize the flow by seeding it with flakes (Irodin 120 Pearl Lustre) and illuminating from above. The visualized image of a mode-3 traveling oscillatory flow is shown in figure 5.2. The white part is where the seeded flakes, lying parallel to the surface, reflected the illumination the most. The deformation of the vortex ring was observed to have a triangular shape which confirms that the azimuthal wave number was three. This method, however, has a disadvantage in detecting wave structures close to criticality, since the deformation of the vortex is very weak in this regime. For this reason, the visualization could not be use to examine the effect of control in the annular flow experiments presented in this thesis.

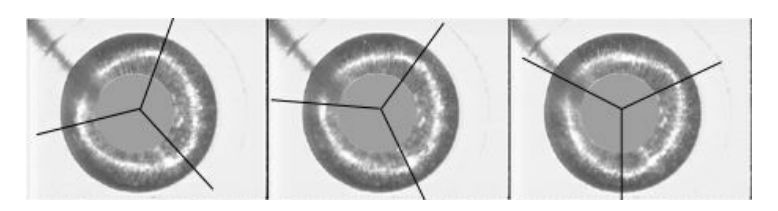


FIGURE 5.2. Top view flow visualization of a mode-3 oscillatory flow in an annular configuration. $(\epsilon, Ma, Ma_{cr}) = (0.6, 70560, 44100)$. Lavalley et al. (2001)

5.4. Toy model formulation

To gain more qualitative understanding of the controlled system, a simple model problem was formulated. Beginning from the Navier-Stokes, energy and continuity equations in the cartigian coordinates, the system is first reduce to disturbance equations solving for the mean flow based on the rough estimation of the spatial profiles. The pressure gradient was ignore in the entire formulation. Now, the idea is to simplify the problem by limiting the number of modes to the base tones and the first harmonics and roughly assuming the spatial profiles of the variables. As shown in Paper 4, by representing the fluctuations of the variables with vector s, the solutions were expanded as.

$$\mathbf{s}(x, y, z, t) = \kappa \{\mathbf{s}_{\mathbf{s}, \mathbf{1}}(t) \sin(2n\pi x) + \mathbf{s}_{\mathbf{c}, \mathbf{1}}(t) \cos(2n\pi x)\} f(y) g(z)$$

$$+ \kappa \{\mathbf{s}_{\mathbf{s}, \mathbf{2}}(t) \sin(4n\pi x) + \mathbf{s}_{\mathbf{c}, \mathbf{2}}(t) \cos(4n\pi x)\} f(y)^{2} g(z)^{2}$$

$$+ \kappa \{\mathbf{s}_{\mathbf{s}, \mathbf{2a}}(t) \sin(4n\pi x) + \mathbf{s}_{\mathbf{c}, \mathbf{2a}}(t) \cos(4n\pi x)\} f(y)^{2} g(z) \frac{dg(z)}{dz}, \quad (5.7)$$

where the profiles of the fluctuations are given as

$$f(y) = \exp(-\frac{y}{\delta'}),\tag{5.8}$$

$$g(z) = 4z(1-z). (5.9)$$

Two types of harmonic spatial modes were considered with different profiles in the direction normal to the free surface to broaden the variation of nonlinear interaction taken into account. This turned to out to be necessary to trigger the oscillatory state. Plugging in these solutions and integrating the system following the idea of weighted residual, we obtain a set of third order ordinary differential equations. The model shows qualitative features that are observed in experiments and numerical simulations such as standing/traveling wave structures and supercritical Hopf bifurcations (figure 5.3).

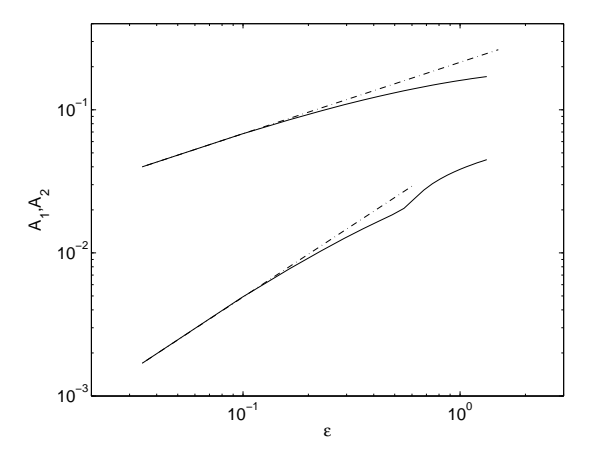


FIGURE 5.3. Supercritical bifurcation in the toy model equation system.

The ultimate goal of the model development is to use it to apply some of the available schemes such as the optimal control theory which requires the system equations to estimate the whole flow field from limited measurement information and to predict the reaction to the control. Although more accurate model would contribute to better prediction of the system, thus better performance of control, full simulation of the Navier-Stokes equations could hardly catch up with the real-time experiment in most of the flow. At this point, it order to realize these control schemes to real application, it may be more practical to use simplified model equations and compensate the loss of resolution of the phenomenon with assumptions based on physical understandings. As shown by Bau & Torrance (1981) for the thermal loop convection, in a low dimensional problem as the current problem, there is a better chance that a simple set of ordinary differential equations can be sufficient, even with fairy strong nonlearity.

5.5. Numerical simulations

5.5.1. Numerical method

A finite element method in the (r, z)-plane combined with a pseudo-spectral method in the azimuthal direction was used to solve the equations in cylindrical coordinates. A Galerkin approach is adopted to formulate the discrete equations. The solutions were expanded to the azimuthal Fourier modes, and for each mode, the equation system is solved, except for the nonlinear terms, in two-dimensional plane using triangular elements with quadratic base function for the velocity and temperature and piecewise linear function for the pressure (P2P1).

The time discretization is done using an Euler implicit and explicit scheme for the viscous terms and nonlinear advection terms, respectively. The pressure is decoupled from the velocity computations by using a projection method. With this implementation, the resulting linear equation system is solved by a conjugate gradient method. The explicit treatment of the convection of the nonlinear terms imposes a restriction on the timestep; a CFL condition needs to be satisfied for numerical stability. The time necessary to simulate one period of oscillation (about one second in physical time) for Ma well over critical value is typically about four hours on a PC with AMD Athlon MP2000.

As mentioned by Leypoldt et al. (2000), this type of problem with azimuthal periodicity is suited to adopt the pseudo-spectral method in the direction. Furthermore, for moderate strength of nonlinearity, the disturbance takes a form of periodic waves with a distinct fundamental wavenumber with its low harmonic modes. In fact, experiments show that even for flow with complex temporal oscillation, the spatial structure of the wave is still low dimension. This allows that the azimuthal structure can be resolved to sufficient accuracy with a limited number of Fourier modes. On computing the nonlinear terms for N_{ϕ} azimuthal planes, de-ailiasing was done by computing the nonlinear terms for $2N_{\phi}$ (r, z) - planes and filtering the first N_{ϕ} modes.

5.5.2. Automated code simulation

The finite element method simulation for two-dimensional flow fields was coded with help from a symbolic coding tool called femLego (Amberg et al. 1999). FemLego is a toolbox in Maple which can generate complete finite element codes. Within the range of utilities of the software, its usability is far from complicated. Using Maple work sheet as an interface, the relevant system equations, Navier-Stokes equations in the current case, are entered into the Maple script, together with the initial and boundary conditions, implicit or explicit solving methods, and optionally output format for post processing. In separate Maple worksheet, the type of finite elements, P2P1 in the present case, is specified. Executing the Maple worksheet, ready-for-compile Fortran 77 code is generated. Together with input parameters and mesh information, the code can be immediately executed.

This tool box enhances the efficiency of the coding process to a large extent. Not only in terms of the initial programing, but mainly in the modification of the code. For example, changes in boundary conditions, dimensions and mathematical model itself can be made simply by changing the Maple script without getting into the related subroutines to make corresponding changes. This would be very beneficial for example in construction of a model equation which best describes the given physics since it would require the try and error routine. In this sense, the benefit of the current study lies in the easy implementation of different controls, in other words, heat flux on the surface free surface.

CHAPTER 6

Summary of results

In this chapter, the context of the papers appended in part 2 is summarized. Instead of listing the summaries of the papers in the order of appearance, the following sections are organized to cover each topics that arose in the course of the entire thesis work. On stating the summary of each topic, results from all the related papers are taken into account.

6.1. Single actuator control

The first experimental attempt was made by applying the proportional control to an annular flow using only one sensor/heater pair (controller). As shown in Paper 1, significant attenuation of the oscillation was achieved in a wide range of supercritical Ma, with the best performance in the weakly nonlinear regime. Quantitative analyses were carried out to characterize the optimal feedback amplification and the required power. Although the attenuation was observed at the sensor position, an uncertainty remained if the global stabilization was indeed achieved in all cases. More detailed measurements with multiple sensors in various azimuthal positions suggested that evaluating the control scheme with single sensor signal could lead us to overestimation of the performance. As reported by Petrov et al. (1998), applying control with single sensor/heater pair could change the initial wave to a standing wave with nodes at the probe positions. Since the oscillation has two degrees of freedom of rotation in the azimuthal direction, at least two controllers are needed to satisfy the controllability. This was confirmed by a numerical investigation (Paper 6).

6.2. Global suppression of the oscillation

The problem stated above was resolved by adding the second controller inheriting the idea of Petrov et al. (1998). The control was experimentally applied in an annular configuration and a half-zone model. In both geometries, significant attenuation of the oscillation was achieved in a range of supercritical Ma and this time, the stabilization was global (Paper 2, 3 and 5). Especially, in the half-zone experiment, the control was performed together with flow visualization and the transitional process of global flow field stabilization was captured. On applying the control, the mode-2 standing wave with the elliptical particle-free area (figure 5.1, a–c) gradually reaches a steady axisymmetric state, as

shown in figure 5.1(d). Radial streaks appear in the particle-free area, which implies that the azimuthal velocity is absent.

In both geometries, the control performs best in the weakly nonlinear regime, where the amplitude of the uncontrolled oscillation is predictable by the weakly nonlinear theory. In this regime, the oscillation could be suppressed to the background noise level as shown in figure 6.1. Having the saturated oscillatory state as the initial condition, with a proper choice of G_1 , the system with the control loop exhibits an exponential decay which clearly indicates that the linear stability of the target mode was modified without influencing the stability of other modes. The heater output plotted bellow shows that, though the output initially overshoots, the power needed to maintain the stabilization is less than 1 mW, which is in the order of a hundredth of the driving power of the base convection. This state could be maintained for infinite time and was quantitatively repeatable. On turning off the control, the fluctuation grows exponentially until it reaches the nonlinear saturation. Similar results were obtained from the numerical simulation of annular flows for the values of ϵ very close to the critical one (Paper 6).

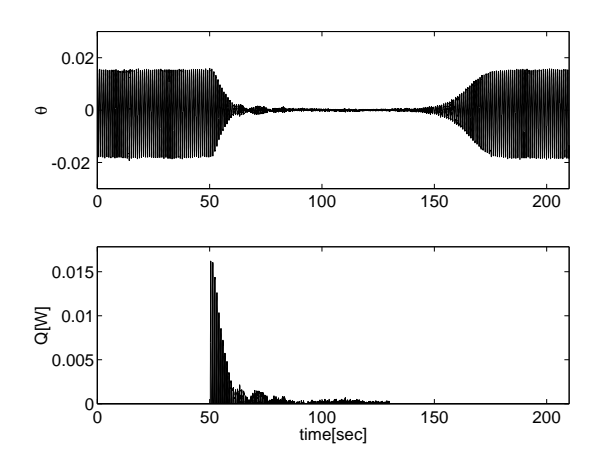


FIGURE 6.1. The typical picture of successful control of oscillation with weakly nonlinearity. Top: Time history of the dimensionless temperature signal. Bottom: Simultaneously measured heater output power. $\epsilon = 0.18$.

6.3. Limitations of control

Although successful suppression of the oscillation was demonstrated for small ϵ , the control also exhibited limitations as nonlinearity becomes stronger. At these values of ϵ , maximum suppression is reduced, where the shortcoming is accompanied with a distortion of the temporal signals. There seems to

be different scenarios causing the limitation, depending on the geometry and configuration of the controllers.

6.3.1. Destabilization of linear modes

It was experimentally observed that, beyond the limitation of control, the time signal exhibits clear modulation which suggests that appearance of other spatial modes with close-by critical frequency as the original one. In the half-zone experiment (Paper 3) the flow visualization captured a clear process of waves with new azimuthal wavenumber (mode), taking the value of 1 for this case, being destabilized. As increasing the linear control gain, the new mode is amplified and eventually dominates the flow as shown in figure 6.2 where excited mode-1 standing wave is visualized.

The results from the annular configuration experiments (Paper 2 and 5) show that the control can amplify both or either of the frequency peaks in the close-by frequency to the fundamental one as in the half-zone experiment, and the first harmonic frequency. For the former case, temperature measurements at multiple locations suggested that the newly appearing oscillation was mode-2. This was confirmed by carrying out a numerical simulation for the annular geometry (Paper 6), where the results show transition from mode-3 to mode-2 dominated flow as increasing the control gain. For the latter case, the toy model shows that an attempt to target the fundamental mode with current local proportional control can result in the destabilization of the first harmonic mode (Paper 4). In the numerical simulation, this type of destabilization was not evident for the limited range of ϵ .

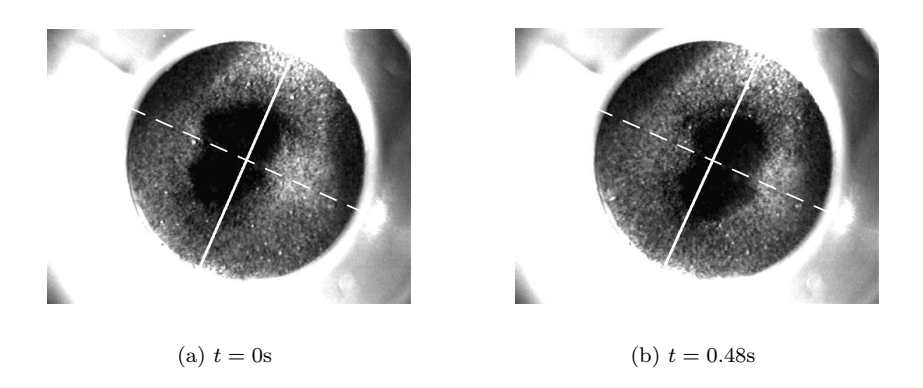


FIGURE 6.2. Flow visualization of excited mode-1 standing wave in a half-zone.

The controlled oscillation always appeared to be a standing wave with nodes nearby sensors and heaters. Therefore, on turning off the control, when the original uncontrolled oscillation has a travelling nature, the symmetry of the problem gives equal possibilities for both clockwise and counterclockwise wave to take over. This could be seen in switch of the direction of rotation before and after applying the control (Paper 2).

6.3.2. Nonlinear limits

The control can certainly enhance nonlinear features of the oscillation. Experiments have shown that an excess of control gain and Ma can result in the broadening of the temporal spectra which would eventually make the state to chaotic. Since the actuation employed in the current control method has definite length, the actuator (or heater) influences a broad range of modes whose width depends on the geometry of the actuator. In spite of our original hope for the generated higher modes to diffuse away, they have a strong influence for high control gain and Ma. As shown in figure 6.3(a), temporal spectra from the experiment in the annular configuration depict the broadening of the peak. Further increase of G_1 forces the system to a chaotic state. The numerical simulation supports these observation where broadening in the spatio-temporal spectra is observed as shown in figure 6.3(b).

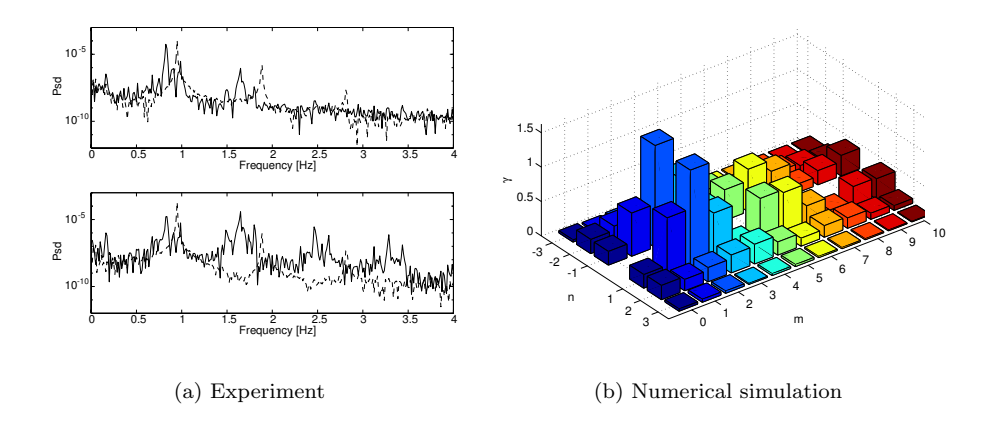


FIGURE 6.3. Broadening of the spectra of the oscillation subjected to the linear control. (a): The temporal spectra of the oscillation without (dashed lines) and with (solid lines) control at $\phi = 0$ (top) and $\phi = \pi/2$ (bottom). Heater length, L_h , is 1.5mm. $\epsilon = 0.24$. (b): The spatio-temporal decomposition of the oscillation in the numerical simulation. γ is the suppression ratio. $\epsilon = 0.07$.

6.4. Remedies

6.4.1. Actuator size

The broadening of the spatio-temporal spectra caused by the local heating can be reduced by increasing the azimuthal length of the actuator. The idea is to attenuate the generation of the broad wavenumber waves in order to reduce the enhancement of nonlinear events. The modification resulted in a significant change in the controlled oscillation where original broad spectra is reduced to clear peaks of two fundamental modes. The change can be observed in the difference between figure 6.3 and 6.4. The limitation of the control is now due to clear destabilization of a linear mode which can be delayed with the following methods. This feature of the controlled oscillation for difference actuator length was also observed in the numerical simulation (Paper 6).

6.4.2. Configuration of the controllers

In case that the limitation of the control is due to the destabilization of a new linear mode, once we have an idea of which mode is amplified, it is possible to delay the destabilization by changing the configuration of the sensors and the actuators. The original series of experiment were carried out with negative G_1 in equation (5.3). Taking the two close-by fundamental modes (original and new) into account, it was suggested that positive G_1 with corresponding changes in the configuration can delay the destabilization of the new modes (Paper 3, 5 and 6).

6.4.3. Weakly nonlinear control

Applying the weakly nonlinear control, the amplitude of the oscillation can be attenuated without altering the linear stability (Ma_{cr}) of the system. The effect can been seen not only for the original critical wavenumber waves but also for the newly appearing mode. This allows us to delay the destabilization of the new mode while attenuating the original mode (Paper 3 and 5). This effect was more evident in the half-zone experiment than the annular one. In the annular configuration, the improvement of the control performance was limited to a slight one. With excess of the control gains, the control does eventually influences the stability characteristics and the transition to the new mode takes place.

6.5. Bifurcation characteristics of the controlled system

The remedies listed above allows us to examine the influence of the control in connection with the bifurcation characteristics. Figure 6.5 shows the resulting bifurcation of mode-2 oscillation subjected to the linear and weakly-nonlinear control in the half-zone experiment. In the experiments with both geometries, clear influences of the linear and cubic control can be observed as described in section 3.5 using the simplest picture of the phenomena. The bifurcation

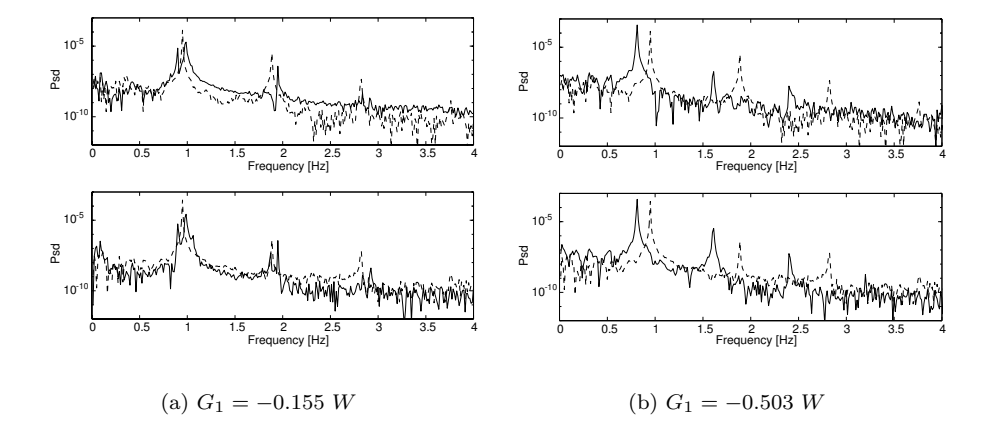


FIGURE 6.4. The power spectrum density for the nondimensional temperature signal for both sensors. Dashed lines: without control. Solid lines: subjected to the linear control with, $G_1 = -0.155~W$ (a) and $G_1 = -0.503~W$ (b). Heater length, $L_h = 1.5mm$. $\epsilon = 0.24$.

analyses for the destabilized mode reveal that the influence of the control on the linear properties of the new mode is not as genuine as the one for the original mode (Paper 3 and 5).

6.6. Controlling the period-doubling oscillation

It is well known that the state becomes chaotic when increasing Ma. In the half-zone experiment, with the strongest technically allowable driving force, the control was applied to the oscillation in a state of period-doubling with period-4 cycle, the beginning of a cascade which leads the system to chaos (Paper 3). On applying the proportional control, as shown in figure 3.3(b), the linear control stabilizes the orbit to a limit cycle. We could attenuate the amplitude of the oscillation by increasing G_1 even more. However, the maximum power output limit of the heater prevented us from exploring the control with optimal values of G_1 .

6.7. Overall performance

The overall performance of the control deduced from the experimental studies in both the annular configuration and the half-zone is shown in figure 6.6. In both geometries, when $\epsilon \ll 1$, the suppression ratio, defined as the ratio of the magnitude of the controlled fluctuation to uncontrolled one, is decreased to the signal to noise ratio. For both cases, γ gradually increases with ϵ with the steepest increment around $\epsilon \sim 0.45$. In overall, a significant attenuation was

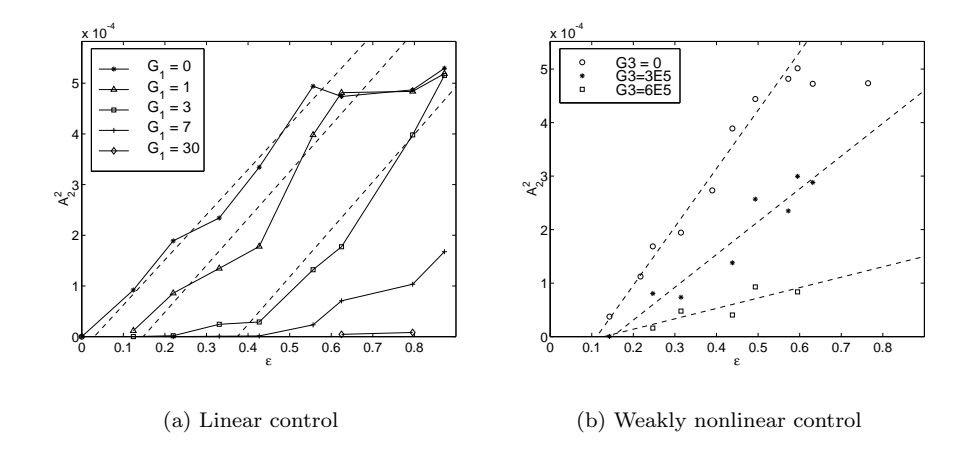


FIGURE 6.5. Bifurcation curves of mode-2 oscillation subjected to the linear and weakly nonlinear control with various control gains. A_2^2 is the squared amplitude. Dotted lines indicate $A_2 \propto \sqrt{\epsilon}$.

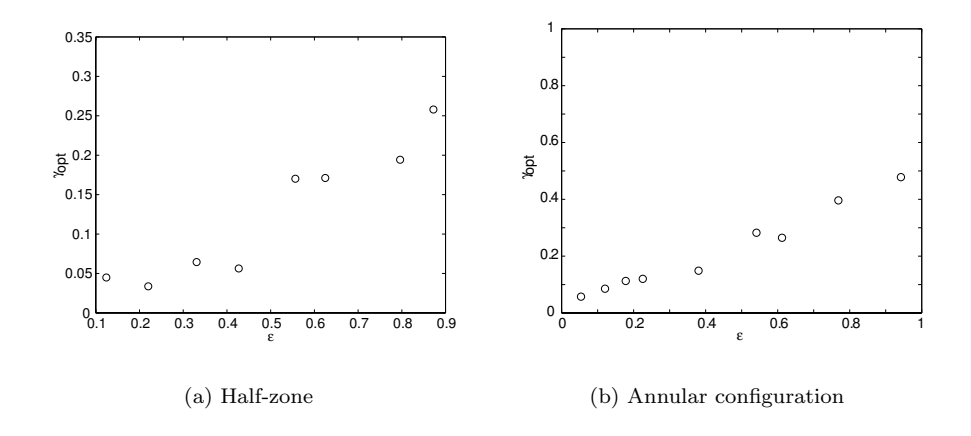


FIGURE 6.6. Overall performance of the proportional control. Circles: suppression ratio γ with the optimal gain $G_{1,opt}$.

observed in a wide range of ϵ (< 1). Comparing the two cases, control shows better performance for the half-zone than for annular geometry. One of the reasons could be due to the higher signal to noise ratio in the half-zone owning to more volatile oscillation.

CHAPTER 7

Conclusions and outlook

The long term goals of the work presented in this thesis concern the possibility to stabilize the thermocapillary instability which gives rise to the oscillation blamed for the detrimental microscopic inhomogeneity in the final product of the crystal growth process. The opposition control presented in this work aims to change the stability characteristics without altering the base flow appreciably. If this can be realized in the real floating-zone crystal growth, there will be an advantage over other base-flow-reducing methods such as applying magnetic field in terms of the macroscopic segregation. Having this as an ultimate goal, the current study has explored the possibility of applying this method in simplified geometries and for high Pr liquids.

The idea originates from Petrov et al. (1996, 1998), where the control is realized by heating or cooling the local free surface by actuators using the feedback control with local sensor signals as inputs. In this study, we proposed a proportional control method where the controllers are strategically placed using the knowledge of the modal flow structures. It was shown that the method can be used to attenuate the oscillation in a range of supercritical Ma. Especially in the weakly nonlinear regime, the control completely suppresses the oscillations. With the right choice of the actuators, even with a local control, it is shown that it is possible to modify the linear and weakly-nonlinear property of the three-dimensional flow system with linear and weakly nonlinear control.

Compared with the scheme of Petrov $et~al.~(1996,\,1998)$, the advantage of the present method lies in its robustness where the control could be carried out in a wide range of $\epsilon~(<1)$ with significant attenuation even when the target state is not reached. Also, the simplicity of the method allowed us to tackle the object without constructing the reference data before hand. In the experiments shown in this thesis, the control gain is manually varied, however, it would be simple to automatically optimize the gain respect to certain objective function as in Bau (1999). In this case, we are left with the dominant azimuthal wavenumber as an open parameter, which can be checked by temperature measurements or flow visualizations. In a well controlled experiment, it could also be reduced from the given aspect ratio.

The actuation of the system using the local boundary heating can also destabilize different mode structures, which increases the dimension of the problem. In the model-independent control schemes using system identification as demonstrated by Petrov *et al.* (1998), one would need twice as many sensors as the number of the active mode in order to maintain the uniqueness of the look-up table, in other word to maintain the observability. Note that we would need two sensors to identify one modal structure. On the other hand, in the current study, having an idea of the newly appearing modes and the fact they are likely to be standing waves, the destabilization can be delayed by optimizing the configuration of sensors and heaters.

In terms of the actuation, the toy model shows that the linear controllability of the system with a fundamental and a harmonic modes can be satisfied by two local heaters. This suggests the possibility that the system may be controlled even with fewer heaters than twice the number of the active modes.

The current study is still limited to high Pr liquids, hence, having the practical application in mind, an important question would be, if this type of control methods is applicable for low Pr system. One obvious doubt is that, since the onset mechanism of the instability in low Pr liquid is a purely hydrodynamical instability, the modification of the thermal field may not have much effect. Furthermore, the heating may have a weak impact on the flow because of a strong thermal diffusion. However, the second bifurcation to the oscillatory state in low Pr flows (Levenstam & Amberg 1995) is not clear yet, and for such a high Ma for which the oscillatory flow is observed, the convective force should have a nontrivial influence in the dynamics. If the heat transport plays a role in the chain of the instability mechanism, surface heating should be sufficient to alter the flow.

On controlling a chaotic state to an oscillatory state, there is still a good chance for a simple control scheme to function. In the low dimensional chaos, the trajectory can still be or comes close to the stable limit cycle, i.e. within the range where linear control can be useful. In fact this could be easier than to suppress a limit cycle to a fix point in a nonlinear system as we do in the oscillation suppression. Although the flow in this regime could not be examined in the current study due to the technical limits of the available experimental apparatuses, it is known that such a chaotic state can be easily achieved by performing the experiment in a freezer (Ueno et al. 2003) which enables us to apply very high driving temperature difference. As shown by Schwabe & Benz (2002), reversing the temperature difference in the annular geometry may do as well.

The validity of the qualitative analyses presented in this work suggests that the experimental system is clean and simple so that, despite of a local control of three dimensional problem, the control problem could be reduced to a lower dimensional model, such as, if all goes well, an ordinary differential equations. Such a simple model as the toy model presented in the current study could recreate many of the features of the controlled system. This encourages the hope for construction of a model system which is sufficiently accurate and simple to be used to realize a control scheme that requires real time computation of the system equation. This may allow us to overcome the limitation of the control performance due to nonlinear dynamics of the system whose influence is inevitable for the current linear control method when Ma is high.

Being a slow phenomenon with a limited number of active modes in the instability and the means of actuation with well-understood influence to the system, the problem may be one of the most suitable problems for experimental realization of the recent development in the art of flow control theories. This problem can be the bridge between two communities of experimental and theoretical control as the problem of thermal convection loop, but with a strong connection with the practical application. I hope that this thesis work will serve as one of the initial studies for such future explorations.

Acknowledgment

First of all, I would like to thank Prof. Gustav Amberg for his warm and enthusiastic support throughout the thesis work. I have been purely amused by how he playfully tackles a problem with his magical physical insights and mathematical skills. Gustav has also brought so much charm to my private life by taking me out to the Swedish wilderness of water.

This work was made only possible with the contribution from the collaborators who are gratefully acknowledged. It was a pleasure working with Masaki Kudo, whose commitment to the experiments made an enormous contribution to the successful collaboration. Ichiro Ueno, my original connection to TUS, has supported me with his charismatic skill to make everybody happy. The encouragement and hospitality of Prof. Hiroshi Kawamura during and ever since my stay at TUS have been extraordinary.

Thanks to Ulf Landén and Marcus Gällstedt who always have a tank full of neat ideas on experimental apparatus with marvelous technical skills to realized them. In the course of the theoretical and numerical works in this thesis, advices and technical supports from Jérôme Hoepffner, Minh Do-Quang and Irina Loginova were very helpful. On finalizing the thesis, contributions were made by Timmy Sigfrids, Thomas Hällqvist, Olle Törnblom, Claes Holmqvist and Henrik Lingman

Special thanks to the international visitors; Nicola Fornaciari, Mikhail Katasonov, Riccardo Ruggeri, Luisa Riparbelli, Richard Forsyth and Luis Bárcena, who have brought a fresh and friendly breeze into the lab.

And with a great importance, thanks to the local gangs; Prof. Henrik Alfredsson and Prof. Masaharu Matsubara for inviting me to KTH, Nils Tillmark for being the *father* of the lab, Prof. Alessandro Talamelli for introducing me to jogging, jazz and g(j)elato, Luca Facciolo and Davide Medici – the club of late-night entrecôte – for being my long-term roommates, Fille Angele, Oso Lindgren and Jens Österlund for all the pints of golden falcon, Veronica Eliasson for the Russian twists, Fredrik Lundell for the rational sailing lectures, Walter Villanueva for painting my boat and the rest of my colleagues for sharing the brightness and darkness of Stockholm-life.

Finally, thanks to Yuko Ozawa, for being the source of my energy and inspiration.

Bibliography

- Amberg, G., Tonhardt, R. & Winkler, C. 1999 Finite element simulation using symbolic computing. *Math. Comput. Simul.* **49**, 257–274.
- ANILKUMAR, A. V., GRUGEL, R. N., SHEN, X. F., LEE, C. P. & WANG, T. G. 1993 Control of thermocapillary convection in a liquid bridge by vibration. J. Appl. Phys 73, 4165–4170.
- AZUMI, T., NAKAMURA, S. & HIBIYA, T. 2001 The effect of oxygen on the temperature fluctuation of Marangoni number convection in a molten silicon bridge. J. Cryst. Growth 223, 116–124.
- Bau, H. H. 1999 Control of Marangoni-Bénard convection. *Intl J. Heat Mass Transfer* **42**, 1327–1341.
- BAU, H. H. & TORRANCE, K. E. 1981 Transient and steady bahavior of an open, symmetrically-heated, free convection loop. Intl J. Heat Mass Transfer 24, 597– 609.
- Benz, S., Hinz, P., Riley, R. J. & Neitzel, G. P. 1998 Instability of thermocapillary–buoyancy convection in shallow layers. Part 2. Suppression of hydrothermal waves. *J. Fluid Mech.* **359**, 165–180.
- CANRIGHT, D. 1994 Thermocapillary flow near a cold wall. Phys. Fluids 6, 1415–1424.
- CHANG, C. E. & WILCOX, W. R. 1976 Analysis of surface tension driven flow in floating zone melting. Intl J. Heat Mass Transfer 19, 355–356.
- CHUN, C. H. & WUEST, W. 1979 Experiments on the transition from the steady to the oscillatory Marangoni-convection of a floating zone under reduced gravity effect. Acta Astron. 6, 1073–1082.
- COWLEY, S. J. & DAVIS, S. H. 1983 Viscous thermocapillary convection at high Marangoni number. J. Fluid Mech. 135, 175–188.
- CRÖLL, A., MÜLLER-SEBERT, W., BENZ, K. W. & NITSCHE, R. 1991 Natural and thermocapillary convection in partially confined silicon melt zones. *Microgravity* sci. technol. 3 4, 204–215.
- Cröll, A., Müller-Sebert, W. & Nitsche, R. 1989 The critical Marangoni number for the onset of time-dependent convection in silicon. *Material Research Bulletin* **24**, 995–1004.
- Cröll, A., Szofran, F. R., Dold, P., Benz, K. W. & Lehoczky, S. L. 1998

- Floating-zone growth of silicon in magnetic fields 2. strong static axial fields. *J. Crys. Growth* **183**, 554–563.
- Cross, M. C. 1988 Structure of nonlinear traveling-wave states in finite geometries. *Phys. Rev. A* 38, 3593–3600.
- DOLD, P., CRÖLL, A. & BENZ, K. W. 1998 Floating-zone growth of silicon in magnetic fields 1. weak static axial fields. J. Crys. Growth 183, 545–553.
- DOLD, P., CRÖLL, A., LICHTENSTEIGER, M., KAISER, T. & BENZ, K. W. 2001 Floating-zone growth of silicon in magnetic fields 4. rotating magnetic fields. J. Crys. Growth 231, 95–106.
- DRESSLER, R. F. & SIVAKUMARAN, N. S. 1988 Non-contaminating method to reduce Marangoni convection in microgravity float zones. J. Crys. Growth 88, 148–158.
- Eyer, A. & Leiste, H. 1985 Striation-free silicon crystals by floating-zoning with surface-coated melt. J. Cryst. Growth 71, 249–252.
- Eyer, A., Leiste, H. & Nitsche, R. 1985 Floating-zone growth of silicon under microgravity in a sounding rocket. *J. Cryst. Growth* 71, 173–182.
- Feigenbaum, M. J. 1978 Quantitative universality for a class of nonlinear transformations. J. Stat. Phys 19, 25.
- FEIGENBAUM, M. J. 1979 The universal metric properties of nonlinear transformations. J. Stat. Phys 21, 69.
- FISCHER, B., FRIEDRICH, J., WEIMANN, H. & MÜLLER, G. 1999 The use of time-dependent magnetic fields for control of convection flows in melt growth configurations. J. Crys. Growth 198, 170–175.
- G. D. ROBERTSON, J. & O'CONNOR, D. J. 1986a Magnetic field effects on float-zone si crystal growth: Ii—. strong axial fields. *J. Crys. Growth* **76**, 111–122.
- G. D. ROBERTSON, J. & O'CONNOR, D. J. 1986b Magnetic field effects on float-zone si crystal growth: Ii. strong transverse fields. J. Crys. Growth 76, 100–110.
- Hibiya, T., Nakamura, S., Sumiji, M. & Azumi, T. 2002 Non-invasive techniques for observing the surface behavior. *J. Cryst. Growth* 237–239, 1854–1858.
- Hosoi, A. E. & Bush, J. W. M. 2001 Evaporative instabilities in climbing films. $\it J.~Fluid~Mech.~{\bf 442},~217-239.$
- HOWLE, L. E. 1997 Control of Rayliegh-Bénard convection in a small aspect ratio container. *Intl J. Heat Mass Transfer* **40**, 817–822.
- Hu, W. R., Shu, J. Z., Zhou, R. & Tang, Z. M. 1994 Influence of liquid bridge volume on the onset of oscillation in floating zone convection. J. Cryst. Growth 142, 379–384.
- IOOSS, G. & JOSEPH, D. D. 1989 Elementary Stability and Bifurcation Theory, 2nd edn. Springer.
- Jurisch, M. 1990 Surface temperature oscillations of a floating zone resulting from oscillatory thermocapillary convection. *J. Crys. Growth* **102**, 223–232.
- JURISCH, M. & LÖSER, W. 1990 Analysis of preiodic non-rotational W striations in Mo single crystals due to nonsteady thermocapillary convection. J. Crys. Growth 102, 214–222.
- Kaiser, T. & Benz, K. W. 1998 Taylor vortex instabilities induced by a rotating magnetic field: A numerical approach. *Phys. Fluids* **10**, 1104–1110.
- KAMOTANI, Y., LEE, J. H., OSTRACH, S. & PLINE, A. 1991 An experimental study

- of oscillatory thermocapillary convection in cylindrical containers. Phys. Fluids A 4, 955–962.
- Kamotani, Y., Masud, J. & Pline, A. 1996 Oscillatory convection due to combined buoyancy and thermocapillarity. *J. Thermophys. Heat Transfer* 10, 102.
- KAMOTANI, Y. & OSTRACH, S. 1998 Theoretical analysis of thermocapillary flow in cylindrical columns of high Prandtl number fluids. J. Heat Transfer 120, 758–764.
- Kamotani, Y., Ostrach, S. & Masud, J. 1999 Oscillatory thermocapillary flows in open cylinderical containers induced by Co₂ laser heating. *Intl J. Heat Mass Transfer* **42**, 555–564.
- Kamotani, Y., Ostrach, S. & Masud, J. 2000 Microgravity experiment and analysis of oscillatory thermocapillary flows in cylindrical container. *J. Fluid Mech.* 410, 211–233.
- KAMOTANI, Y., OSTRACH, S. & PLINE, A. 1995 A thermocapillary convection experiment in microgravity. J. Heat Transfer 117, 611–618.
- KAWAMURA, H., UENO, I. & ISHIKAWA, T. 2002 Study of thermocapillary flow in a liquid bridge towards an on-orbit experiment aboard the International Space Station. *Adv. Space Res.* **29**, 611–618.
- KAZARINOFF, N. D. & WILKOWSKI, J. S. 1989 A numerical study of Marangoni flows in zone-refined silicon crystals. *Phys. Fluids A* 1, 625.
- KAZARINOFF, N. D. & WILKOWSKI, J. S. 1990 Bifurcation of numerically simulated thermocapillary flows in axially symmetric float zones. *Phys. Fluids A* 2, 1797.
- KIMURA, H., HARVEY, M. F., O'CONNER, D. J., ROBERTSON, G. D. & VALLEY, G. C. 1983 Magnetic field effects on floating-zone Si crystal growth. J. Crys. Growth 62, 523–531.
- KUHLMANN, H. C. 1998 Thermocapillary convection. In Free surface flows (ed. H. C. Kuhlmann & H. J. Rath), pp. 145–207. Springer.
- Kuhlmann, H. C. & Rath, H. J. 1993 Hydrodynamic instabilities in cylindrical thermocapillary liquid bridges. J. Fluid Mech. 247, 247–274.
- LAN, C. W. & Kou, S. 1991a Floating-zone crystal growth with a heated and immersed shaper experiments. J. Cryst. Growth 108, 541–548.
- LAN, C. W. & KOU, S. 1991b Floating-zone crystal growth with a heated ring covering the melt surface. J. Cryst. Growth 108, 1–7.
- LAVALLEY, R., AMBERG, G. & ALFREDSSON, H. 2001 Experimental and numerical investigation of nonlinear thermocapillary oscillations in an annular geometry. *Eur. J. Mech. B/Fluids* **20**, 771–797.
- LEE, C. P. 1998 The balancing of thermocapillary flow in a floating zone by ripple-driven streaming. *Phys. Fluids* 11, 2765–2780.
- Lee, C. P., Anilkumar, A. V. & Wang, T. G. 1996 Streaming generated in a liquid bridge due to nonlinear oscillations driven by the vibration of an endwall. *Phys. Fluids* 8, 3234–3246.
- Leon, N. D., Guldberg, J. & Salling, J. 1981 Growth of homogeneous high resistivity FZ silicon crystals under magnetic field bias. *J. Crys. Growth* **55**, 406–408.

- Levenstam, M. & Amberg, G. 1995 Hydrodynamical instabilities of thermocapillary flow in a half-zone. *J. Fluid Mech.* **297**, 357–372.
- Levenstam, M., Amberg, G. & Winkler, C. 2001 Instabilities of thermocapillary convection in a half-zone at intermediate Prandtl numbers. *Phys. Fluids* 13, 807–816.
- LEYPOLDT, J., KUHLMANN, H. C. & RATH, H. J. 2000 Three-dimensional numerical simulation of thermocapillary flows of cylindrical liquid bridges. *J. Fluid Mech.* 414, 285–314.
- LIBCHABER, A., LAROCHE, C. & FAUVE, S. 1982 Period doubling cascade in mercury, a quantitative measurement. J. Physique Lett. 43, 211.
- MASUD, J., KAMOTANI, Y. & OSTRACH, S. 1997 Oscillatory thermocapillary flow in cylindrical columns of high prandtl number fluids. *J. Thermophys. Heat Tr.* 11, 105–111.
- MONTI, R., FORTEZZA, R., CASTENUTO, D. & DESIDERS, G. 1994 The telemaxus experiment on oscillatory Marangoni flow. ESA SP 1132 4, 44.
- Neitzel, G. P., Chang, K. T., Jankowski, D. F. & Mittelmann, H. D. 1993 Linear stability theory of thermocapillary convection in a model of the float-zone crystal-growth process. *Phys. Fluids A* 5, 108–114.
- OR, A. C. & Kelly, R. E. 2001 Feedback control of weakly nonlinear Rayleigh-Bénard-Marangoni convection. *J. Fluid Mech.* **440**, 27–47.
- OR, A. C., KELLY, R. E., CORTELEZZI, L. & SPEYER, J. L. 1999 Control of long-wavelength Marangoni-Bénard convection. J. Fluid Mech. 387, 321–341.
- Ott, E., Grebogi, C. & Yorke, J. A. 1990 Controlling chaos. *Phys. Rev. Lett.* **64**, 1196–1199.
- Pearson, J. R. A. 1958 On convection cells included by surface tension. *J. Fluid Mech.* 4, 498–500.
- Petrov, V., Muehlner, K. A., Vanhook, S. J. & Swinney, H. L. 1998 Model-independent nonlinear control algorithm with application to a liquid bridge experiment. *Phys. Rev. E* 58, 427–433.
- Petrov, V., Schatz, M. F., Muehlner, K. A., Vanhook, S. J., McCormick, W. D., Swift, J. B. & Swinney, H. L. 1996 Nonlinear control of remote unstable states in a liquid bridge convection experiment. *Phys. Rev. Lett.* 77, 3779–3782.
- PFANN, W. G. 1966 Zone Melting, 2nd edn. John Wiley & Sons, Inc.
- Preisser, F., Schwabe, D. & Scharmann, A. 1983 Steady and oscillatory thermocapillary convection in liquid columns with free cylindrical surface. *J. Fluid Mech.* 126, 545–567.
- RILEY, R. J. & NEITZEL, G. P. 1998 Instability of thermocapillary-buoyancy convection in shallow layers. Part 1. Characterization of steady and oscillatory instabilities. J. Fluid Mech. 359, 143.
- ROSENBLAT, S., DAVIS, S. H. & HOMSY, G. M. 1982a Nonlinear Marangoni convection in bounded layers. part 1. circular cylindrical containers. *J. Fluid Mech.* 120, 91–122.

- ROSENBLAT, S., HOMSY, G. M. & DAVIS, S. H. 1982b Nonlinear Marangoni convection in bounded layers. part 2. rectangular cylindrical containers. *J. Fluid Mech.* 120, 123–138.
- SAVINO, R. & MONTI, R. 1996 Oscillatory Marangoni convection in cylindrical liquid bridges. Phys. Fluids 8, 2906–2922.
- Schatz, M. F. & Neitzel, G. P. 2001 Experiments on thermocapillary instabilities. *Annu. Rev. Fluid Mech.* **33**, 93–127.
- SCHWABE, D. & BENZ, S. 2002 Thermocapillary flow instabilities in an annulus under microgravity – results of the experiment MAGIA. Adv. Space Res. 4, 629–638.
- Schwabe, D., Hintz, P. & Frank, S. 1996 New features of thermocapillary convection in floating zones revealed by tracer particles accumulation structures (PAS). *Microgravity Sci. Technol.* **9**, 163–168.
- Schwabe, D., Möller, U., Schneider, J. & Scharmann, A. 1992 Instabilities of shallow dynamic thermocapillary liquid layers. *Phys. Fluids* 4, 2368.
- Schwabe, D. & Scharmann, A. 1979 Some evidence for the existence and magnitude of a critical Marangoni number for the onset of oscillatory flow in crystal growth melts. *J. Cryst. Growth* 6, 125–131.
- Schweizer, M., Cröll, A., Dold, P., Kaiser, T., Lichtensteiger, M. & Benz, K. 1999 Measurement of temperature fluctuations and microscopic growth rates in a silicon floating zone under microgravity. *J. Crys. Growth* **203**, 500–510.
- SCRIVEN, L. E. & STERNLING, V. 1960 The Marangoni effects. Nature 187, 186–188.
- Shen, X. F., Anilkumar, A. V., Grugel, R. N. & Wang, T. G. 1996 Utilizing vibration to promote microstructural homogeneity during floating-zone crystal growth processing. *J. Crys. Growth* **165**, 438–446.
- SIM, B.-C. & ZEBIB, A. 2002 Effect of free surface heat loss and rotation on transition to oscillatory thermocapillary convection. *Phys. Fluids* **14**, 225–231.
- SMITH, M. K. 1986 Instability mechanism in dynamic thermocapillary liquid layers. Phys. Fluids 29, 3182–3186.
- SMITH, M. K. 1988 The nonlinear stability of dynamic thermocapillary liquid layers. J. Fluid Mech. 194, 391–415.
- SMITH, M. K. & DAVIS, S. H. 1983 Instability of dynamic thermocapillary liquid layers. J. Fluid Mech. 132, 119.
- Strogatz, S. H. 1994 Nonlinear dynamics and chaos, 1st edn. Preseus Books Publishing, LLC.
- SUMIJI, M., NAKAMURA, S. & HIBIYA, T. 2002 Two-directional observation of solid-melt interface fluctuation induced by Marangoni flow in a silicon liquid bridge. J. Cryst. Growth 235, 55–59.
- Tang, J. & Bau, H. H. 1993 Feedback control stabilization of the no-motion state of a fluid confined in a horizontal, porous layer heated from below. *J. Fluid Mech.* **257**, 485–505.
- TANG, J. & BAU, H. H. 1998 Experiments on the stabilization of the no-motion state of a fluid layer heated from below and cooled from above. J. Fluid Mech. 363, 153–171.
- Thomson, J. 1855 On certain curious motions observable at the surface of wine. *Phil.* Maq. 10, 330–333.

- Ueno, I., Tanaka, S. & Kawamura, H. 2003 Oscillatory and chaotic thermocapillary convection in a half-zone liquid bridge. *Phys. Fluids* **15**, 408–416.
- VELTEN, R., SCHWABE, D. & SCHARMANN, A. 1991 The periodic instability of thermocapillary convection in cylindrical liquid bridges. Phys. Fluids A 3, 267–279.
- VUILLEUMIER, R., EGO, V., NELTNER, L. & CAZABAT, A. M. 2001 Evaporative instabilities in climbing films. J. Fluid Mech. 442, 217–239.
- WANG, Y., SINGER, J. & BAU, H. H. 1992 Controlling chaos in a thermal convection loop. J. Fluid Mech. 237, 479–498.
- Wanschura, M., Shevtsova, V. M., Kuhlmann, H. C. & Rath, H. J. 1995 Convective instability mechanisms in thermocapillary liquid bridges. *Phys. Fluids* 7, 912–925.
- WIENER, R. J., SNYDER, G. L., PRANGE, M. P., FREDIANI, D. & DIAZ, P. R. 1997 Period-doubling cascade to chaotic phase dynamics in taylor vortex flow with hourglass geometry. *Phys. Rev. E* 55, 5489–5497.
- Yuen, P. K. & Bau, H. H. 1996 Rendering a subcritical Hopf bifurcation supercritical. *J. Fluid Mech.* 317, 91–109.
- ZIEF, M. & WILCOX, W. R. 1967 Fractional solidification, 1st edn. Marcel Dekker Inc.